surface. The central fragment, before being shed to the medium, is further processed to 50 kDa and 6 kDa fragments [12–14]. Several protease inhibitors have been identified to block proteolytic processing of Pfa-SERA5 resulting to a developmental arrest at schizont rupture/merozoite release [13]. Pfa-SERA5 processing is mediated by a subtilisin-like serine protease called PfSUB1 and the inhibition of this processing, likewise, results in blockade of merozoite release [15,16]. The precise molecular mechanism(s) of parasite egress from an infected erythrocyte, however, remains to be determined.

Previous evolutionary studies of SERA genes from eight *Plasmodium* species have shown that these can be categorized into Groups I to IV, according to gene structure and phylogenetic relatedness [17]. Groups I to III and Group IV SERA genes encode proteins with protease motif that either have cysteine or serine residue, respectively, in the catalytic site. The SERA multigene family of *P. falciparum* (Pfa-SERA1 to Pfa-SERA8) is clustered head-to-tail on chromosome 2 between a conserved hypothetical protein (HP) gene and a putative iron-sulfur assembly protein gene (hesB) [3]. Another SERA gene, Pfa-SERA9, is located on chromosome 9. The gene synteny of the clustered SERA multigene family is conserved among *Plasmodium* species examined, except for SERA3 of *P. gallinaceum*, an avian parasite [17]. The number of SERA genes in the clustered region varies among parasite species, from two in *P. gallinaceum* to 12 in *P. vivax*, the benign human malaria parasite. Outside the genus *Plasmodium*, no apicomplexan parasite has a SERA ortholog, except *Theileria*, a closely related protozoan parasite of cattle, which has one SERA ortholog [17]. The evolutionary process of the *Plasmodium* SERA multigene family, however, remains largely unknown. Also, no study has been done for SERA multigene families of human malaria parasites, *P. malariae* and *P. ovale*; and *P. vivax*-related monkey malaria parasites. Since *P. vivax* became a human parasite by host switch from a monkey parasite, it is worth to see whether *P. vivax* SERA gene family underwent unique evolution, distinctive from closely related monkey parasites.

In this study, in our attempt to unravel the evolutionary history of the SERA gene family of *Plasmodium*, we newly determined SERA genes from 11 primate *Plasmodium* species: nine *P. vivax*-related monkey parasites; and *P. malariae* and *P. ovale*. Together with previously reported SERA sequences, we performed evolutionary analyses of the gene family. Results obtained here show that the number of SERA genes remarkably differs among parasite lineages and the variation in mammalian parasites was found only in serine-type SERA gene but not in cysteine-type SERA gene. We noted that the gene number variation occurred lineage-specifically, which was particularly evident in human, ape and monkey parasite groups. In addition, we found that transcription of individual SERA genes varied greatly among rodent and monkey parasites, supporting lineage-specific evolution of the *Plasmodium* SERA gene family.

Results

Arrangement of SERA multigene family in 18 *Plasmodium* species

The 18 *Plasmodium* species analyzed in this study and their natural hosts are: *P. falciparum*, *P. vivax*, *P. malariae* and *P. ovale* (humans); *P. reichenowi* (chimpanzees); *P. gonderi* (African Old World monkeys); *P. fragile*, *P. coatneyi*, *P. knowlesi*, *P. inui*, *P. fieldi*, *P. simiovale*, and *P. cynomolgi* (Asian Old World monkeys), *P. hylobati* (gibbons), *P. yoelii*, *P. berghei* and *P. chabaudi* (rodents); and *P. gallinaceum* (birds) [Underline denotes newly determined SERA sequences in this study]. *P. vivax* is closely related to Asian Old World monkey parasites [18]. Additionally, it should be mentioned that primate malaria parasites are phylogenetically classified into two distinct groups: group 1 for *P. falciparum* and *P. reichenowi*; and group 2 for *P. malariae*, *P. ovale*, *P. vivax* and the nine Old World monkey parasite species [19,20]. A total of 116 new SERA gene sequences, of which 11 and 18 are truncated genes and pseudogenes, respectively (Table 1 and Figure S1) were analyzed together with 47 SERA genes previously published from seven *Plasmodium* species (Table 1 and Figure S1). Details of SERA genes, truncated genes and pseudogenes are described in Figure S1. A SERA gene map that follows the genomic organization of the genes is shown in Figure 1.

Almost all SERA genes were clustered between two conserved genes; a conserved hypothetical protein (HP) gene and the iron-sulfur assembly protein gene (hesB) (Figure 1 and Figure S1). Except for one SERA gene from *P. falciparum*, *P. reichenowi* and *P. gallinaceum* that are located outside the clustered region, all SERA genes lie disposed head-to-tail on the chromosomes where they were found. The number of SERA genes in the cluster varied from 2 (*P. gallinaceum*) to 12 (*P. vivax*) among 18 *Plasmodium* species. All parasite species have one SERA gene from Group I, Group II and Group III (cysteine-type SERA gene), with the exception of *P. gallinaceum*, which has only two SERA genes, one from Group I and the other from a common ancestor of Groups II and III (Figure 2). Thus, the difference in the number of SERA genes among the 17 *Plasmodium* species lies in Group IV (serine-type SERA gene). Likewise, while orthologous relationship of SERA genes in Groups I to III were readily identified from sequence similarity and phylogenetic analysis (Figure 1 and Figure 2), the relationship was identified only for some (but not all) SERA genes in Group IV (Figure 1, orthologous gene groups supported by phylogenetic analyses (below) are indicated by vertical dashed-lines). The high divergence of SERA genes including variations in gene number was notable only in Group IV SERA genes in mammalian malaria parasites. In particular, the number of Group IV SERA genes remarkably increased in two primate parasite lineages.

Primary structure of SERA genes

The SERA gene family has a common exon/intron structure: four exons and three introns, with few exceptions. SERA genes of Group I have six exons and five introns structure, except for Pfa-SERA8 and Pvi-SERA12, which lack one intron. Other exceptions are detailed in Figure 1. Pcy-SERA3 was closely related to Pcy-SERA5 but not to Pvi-SERA3 (Figure 2), and Pco-SERA1 showed a fusion of exon 3 and 4, which is similar to Pco-SERA2 (Figure 1). These genes were generated probably by gene conversion between Pcy-SERA3 and Pcy-SERA5, and Pco-SERA1 and Pco-SERA2, respectively. SERA was originally named after tandem repeats of serine residues in Pfa-SERA5 (and Pre-SERA5, an ortholog of Pfa-SERA5) [21]. Here, we found 47 tandem repeats of serine in Pma-SERA8. The position of serine repeats was, however, markedly different between Pma-SERA8 (in variable domain 2) and Pfa-SERA5/Pre-SERA5 (in variable domain 1) (Figure S2).

Amino acid sequence alignments reveal the consensus primary structure of SERA genes (Figure 3A, % similarity is color coded). Downstream of the signal peptide sequence at the N-terminus, is a sequence region (variable domain 1), in which extensive sequence variations are found among parasite species. At the central domain of Pfa-SERA5, functional genetic and structural analyses identified the pro-enzyme and enzyme domain [22,23], flanked by the reported PfSUB1 cleavage sites [15]. Pfa-SERA4 (Group IV) and Pfa-SERA6 (Group II) were likewise cleaved by recombinant PfSUB1 [15].

Table 1. Summary of the *Plasmodium* SERA genes determined and analyzed in this study.

Species (strain[a])	SERA gene	Truncated SERA gene	Fragmented or Pseude SERA gene	Accession number (bp)
P. malariae (Kisii67)	10	0	3	AB576870 (66,408)
P. ovale (Nigeria II)	7	0	1	AB576871 (45,833)
P. cynomolgi (Mulligan)	11	1	2	AB576872 (67,118)
P. fieldi (N-3)	9	1	2	AB576873 (56,691)
P. simiovale	9	1	2	AB576874 (56,056)
P. inui (Celebes)	7	1	4	AB576875 (53,234)
P. hylobati (WAK)	7	1	0	AB576876 (41,987)
P. coatneyi (CDC)	7	2	1	AB576877 (44,850)
P. knowlesi (H)	6	2	0	AB576878 (40,735)
P. fragile (Hackeri)	5	2[b]	2	AB576879 (34,519)
P. gonderi	9	0	1	AB576880+AB576881 (22,367+27,149)
P. vivax (SalI)	12	1	1	See Table S2
P. berghei (ANKA)	5	0	0	See Table S2
P. yoelii (17NXL)	5	0	0	See Table S2
P. chabaudi (AS)	5	0	0	See Table S2
P. falciparum (3D7)	9	0	0	See Table S2
P. reichenowi (Oscar)	8[c]	0	0	Ref. 17
P. gallinaceum	3	0	0	Ref. 17

[a]ATCC numbers: P. cynomolgy = 30155, P. fieldi = 30163, P. simiovale = 30104, P. hylobati = 30154, P. knowlesi = 30158, P. gonderi = 30045.
[b]One of two truncated SERA genes is also a putative pseudogene.
[c]SERA gene sequences of P. reichenowi is not complete.
doi:10.1371/journal.pone.0017775.t001

The consensus sequence of the cleavage site is (Val/Leu/Ile)-Xaa-(Gly/Ala)-Paa, in which Xaa is any amino acid residue and Paa is a non-polar residue except for Leu [15]. The consensus sequence is well conserved with slight modifications in all Group II to IV *Plasmodium* SERA genes analyzed here (Figure S2). In the C-terminal region, there occur interspecies variable sequence region (variable domain 2) and interspecies conserved sequence region, in which 7 cysteine residues are perfectly conserved in all SERA genes (Figure S2). Degenerating oligopeptide tandem repeats were found in both variable domains 1 and 2. Group I SERA genes lack most of the N-terminal variable domain 1 and SUB1 cleavage sites.

Amino acid sequence variations of Groups I to IV SERA genes varied greatly among parasite lineages (Figure 3B), with the highest variation in *P. vivax* and related monkey malaria parasite lineage. In *P. falciparum* and *P. reichenowi*, sequences are highly conserved in all domains of Groups I to IV, except for Group IV variable domains 1 and 2. In rodent parasite lineage, sequences are somewhat variable in the two variable domains of Groups I to IV, but relatively conserved in both the putative pro-enzyme and enzyme domains. In *P. vivax* and related monkey parasites, putative pro-enzyme and putative enzyme domains remains relatively conserved compared to two variable domains whose sequence variations are very high. Thus, overall, although putative pro-enzyme and putative enzyme domains seem fairly conserved, the extent of variation in variable domains 1 and 2 differs greatly among parasite lineages.

Phylogenetic analyses of *Plasmodium* SERA genes

The maximum likelihood (ML) phylogenetic tree was constructed from 134 SERA genes representing 18 *Plasmodium* species, using 392 unambiguously aligned amino acid sites (Figure S3). The best tree shows that genes were categorized into four major groups, Groups I to Group IV. The monophyletic grouping of Group I SERA genes is supported with 100% bootstrap value. The long internal branch separating Group I from Groups II to IV suggests that the root of the tree is located on the branch leading to the common ancestor of the Group I SERA genes. It is thus likely that Group I genes have appeared early in the evolution of SERA gene family, being consistent with our previous analysis [17].

To enhance/increase the resolution of the ML tree, the long branched Group I genes were excluded from analysis and the ML phylogenetic tree was constructed from 115 Group II to Group IV SERA genes using 570 amino acid sites. The monophyletic grouping of Group II, III and IV SERA genes is supported by 82%, 95% and 100% bootstrap values, respectively (Figure 2). Group IV SERA genes, which diverged after the substitution of cysteine to serine in the catalytic site of the cysteine protease motif, were further categorized to five monophyletic sub-Groups: (i) *P. falciparum* and *P. reichenowi*, (ii) rodent *Plasmodium* species, (iii) *P. ovale*, (iv) *P. malariae* and (v) *P. vivax* and *P. vivax*-related monkey parasite species (Figure 2). Closer examination of these sub-groups revealed several notable features. First, in lineages which contain multiple parasite species, internal branches form sub-lineages, from which orthologous relationship of SERA genes are evident. For example, in three rodent parasites, SERA1 genes and SERA2 genes are separable with 100% bootstrap value. Similar separations can be seen in lineages of *P. falciparum*/*P reichenowi*, and *P. vivax* and related monkey parasites. These indicate that Group IV SERA genes were duplicated independently in each of the three sub-group lineage: *P. falciparum*/*P. reichenowi*, rodent parasites, and *P. vivax* and related monkey parasites.

Group IV SERA genes of *P. vivax* and *P. vivax*-related monkey parasites (10 species) were further categorized into six orthologous

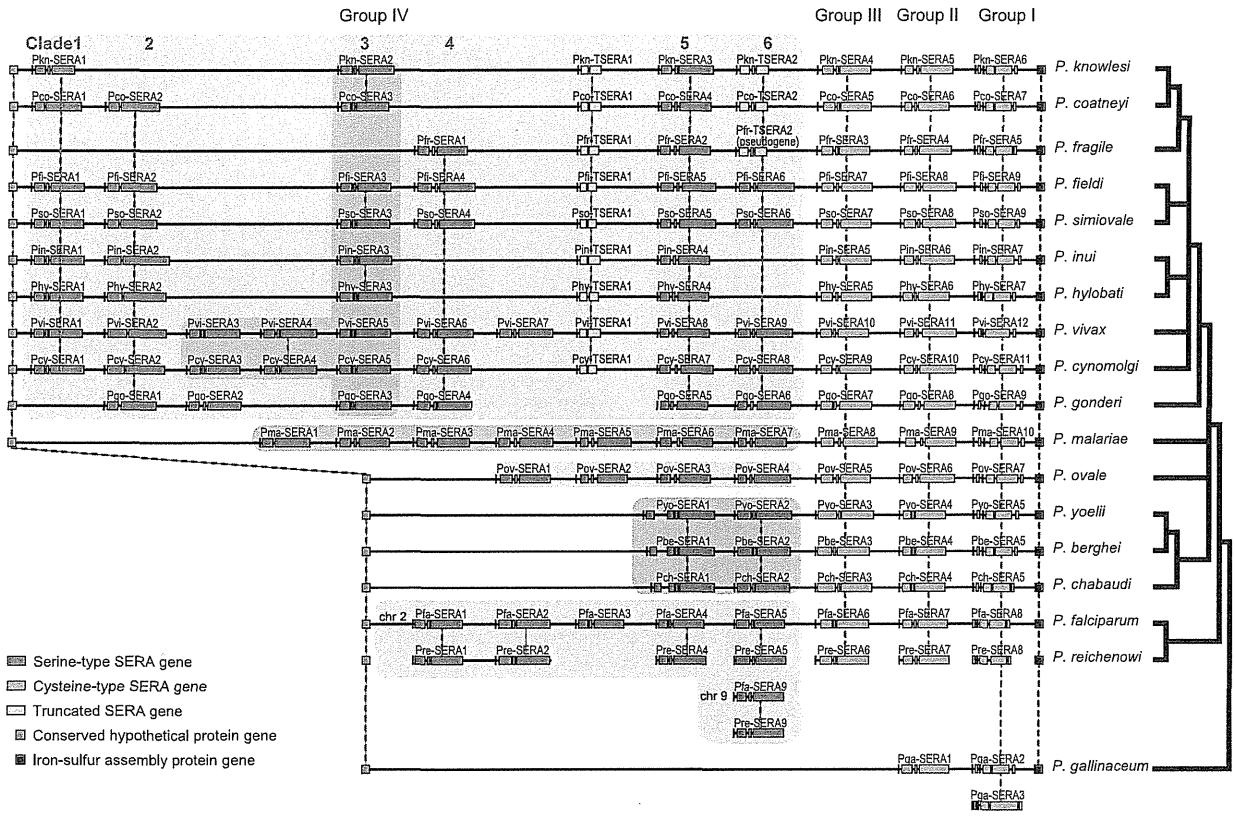

Figure 1. The organization of the SERA gene family in 18 *Plasmodium* species. SERA genes are arrayed onto a solid horizontal line for each parasite species. Gene arrangement follows the genomic organization in each species. Individual SERA genes are clustered between a conserved hypothetical gene and the iron-sulfur assembly protein gene. Pfa-SERA9, Pre-SERA9 and PgaSERA3 have aberrant locations. SERA genes were categorized to Groups I to IV and Clades 1 to 6 reflecting orthologous gene groups as inferred from phylogenetic analyses shown in Figure 2 and Figure S3. SERA genes of Groups I to III (cysteine-type SERA gene) and those of Group IV (serine-type SERA gene) are shown in green and blue, respectively. TSERA denotes truncated SERA genes shown in yellow. SERA genes are drawn to scale, but other genes and intergenic regions are not. Dashed lines and/or dark gray boxes denote orthologous relationships. A generally accepted consensus phylogenetic tree of *Plasmodium* species is shown in right. The abbreviations for species names are: *P. falciparum* (Pfa), *P. vivax* (Pvi), *P. malariae* (Pma), *P. ovale* (Pov), *P. reichenowi* (Pre), *P. gonderi* (Pgo), *P. fragile* (Pfr), *P. coatneyi* (Pco), *P. knowlesi* (Pkn), *P. inui* (Pin), *P. fieldi* (Pfi), *P. simiovale* (Pso), *P. cynomolgi* (Pcy), *P. hylobati* (Phy), *P. yoelii* (Pyo), *P. berghei* (Pbe), *P. chabaudi* (Pch), and *P. gallinaceum* (Pga). The SERA gene family has common exon/intron structure: four exons and three introns, with some exceptions. Group I SERA genes have six exons and five introns structure, except for Pfa-SERA8 and Pvi-SERA12, which lack one intron. SERA genes of Group IV Clade 2 and Pma-SERA1 have no third intron and consist of three exons and two introns. Group I SERA genes of three rodent parasites have an extra intron near the 5′-end. Pkn-SERA1 gene in Clade 1 contains three stop codons, causing truncation of the cysteine-rich conserved domain; but since this gene was expressed, we consider this is a SERA gene. TSERA1 genes have truncations of the protease domain, variable domain 2 and cysteine-rich conserved domain. Pco-TSERA2, Pkn-TSERA2 and Pfr-TSERA2 lack a long amino acid region (498 residues) including the enzyme domain (Figure S4), of which Pfr-TSERA2 seems to be a putative pseudogene because its 2nd exon contains two stop codons.
doi:10.1371/journal.pone.0017775.g001

gene groups (Clade 1 to Clade 6), except for Pgo-SERA2 and Pvi-SERA7 (Figure 2). The number of SERA genes varies from 5 (*P. fragile*) to 12 (*P. vivax*). Orthologous relationships of the SERA genes and their locations are shown in Figure 4. Each clade has 5 (Clade 6) to 10 (Clade 5) parasite species. This does suggest that a common ancestor of *P. vivax* and related monkey malaria parasites had at least 6 SERA genes of Group IV, followed by gene duplications and gene deletions in each lineage. Pgo-SERA2 and Pvi-SERA7 have no orthologous genes. Pgo-SERA2 was located at the earliest branching position in Group IV SERA genes (Figure 2). An ortholog of Pgo-SERA2 was possibly lost in a common ancestor of Asian Old World monkey parasites, after divergence from a common ancestor of African and Asian Old World monkey parasites. Although Pvi-SERA7 has no ortholog in other species, several parasite species have a SERA gene fragment just upstream of TSERA1 (Figure 4), which is similar to Pvi-SERA7. Since we failed to obtain *P. gonderi* sequences corresponding to Pvi-SERA7 and TSERA1 orthologs, we cannot infer further on the origin of these genes. In Group IV, there are notably many SERA gene fragments and pseudogenes containing multiple stop codons. Taken together, extensive gene duplications, gene deletions as well as pseudogenization/truncation are evident in the serine type SERA gene (Group IV) of *P. vivax* and related monkey malaria parasites.

Transcription analysis of SERA gene

Transcription of SERA genes was analyzed for the late trophozoite to schizont stages of the rodent parasite, *P. berghei*, and monkey parasites *P. knowlesi*, *P. cynomolgi* and *P. coatneyi*. The amount of each SERA gene transcript is presented relative to that of β-tubulin in Figure 5. In *P. berghei*, Pbe-SERA3 (Group III SERA gene) was predominantly expressed followed to a lesser

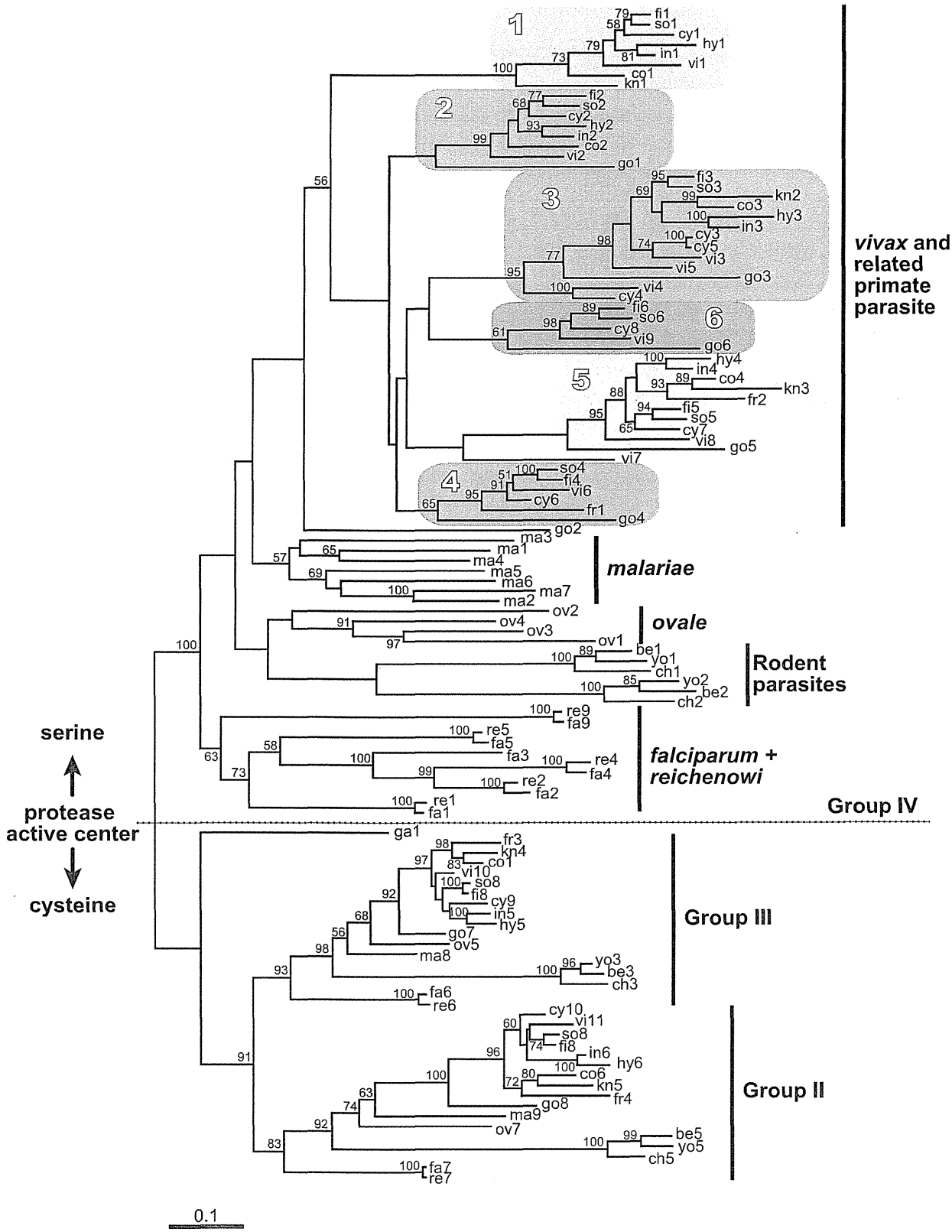
1
2
3
4
5
6
vivax and related primate parasite
malariae
ovale
Rodent parasites
falciparum + reichenowi
Group IV
Group III
Group II
serine
protease active center
cysteine
0.1

Figure 2. The maximum likelihood (ML) phylogenetic tree of *Plasmodium* SERA genes. This unrooted tree was constructed from 115 SERA genes (encompassing Groups II to IV, see Figure 1) using 570 amino acid positions under the JTT + Γ (eight categories) model (α = 1.15) with 500 heuristic replicates. Bootstrap proportions >50% are shown along nodes. Groups II - III and Group IV are cysteine-type and serine-type SERA genes, respectively. Note that Pga-SERA1 (ga1) is an offshoot of Groups II and III SERA genes, suggesting the occurrence of a common ancestor, leading to Pga-SERA1 (ga1) and a common ancestor of Group II and Group III. In *P. vivax* and *P. vivax*-related monkey malaria parasite species, the six clades are color-boxed. Pgo-SERA1 (go1) and Pgo-SERA5 (go5) were grouped, despite low bootstrap values, into Clade 2 and Clade 5 respectively, because these genes showed common features to each clade in exon/intron structure and/or gene array.
doi:10.1371/journal.pone.0017775.g002

extent by other SERA genes except for SERA 5 that did not show detectable expression. In three monkey parasites, the abundantly expressed genes are members of Group IV Clade 3: Pcy-SERA3 and Pcy-SERA5, Pco-SERA3 and Pkn-SERA2. Other SERA genes of Group IV, except Pcy-SERA1 and Pco-SERA1, were also expressed to varying degrees. All Group III SERA gene expression was evident; whereas, no expression was observed for all Group I SERA genes. From above, SERA genes were differently expressed between rodent and primate parasites, with the exception of Group I SERA genes, which were not expressed at the blood stage parasites of both *P. berghei* and three monkey parasites.

Discussion

This study presents an overview of the evolution of the *Plasmodium* SERA gene family (Figure 6). Since the genus *Theileria*, closely related to *Plasmodium*, has only one SERA gene of the cysteine-type, it is inferred that cysteine-type SERA gene initially duplicated in a common ancestor of all *Plasmodium* species. One of the duplicated genes became a common ancestor of a SERA gene of Groups II and III. Another duplication took place in a lineage leading to *P. gallinaceum* to form two SERA genes of Group I. In a common mammalian malaria parasite ancestor, the common ancestral SERA gene was duplicated which subsequently generated two cysteine-type SERA genes (Group II and Group III). Following divergence of mammalian malaria parasite species, a lineage leading to *P. falciparum* and *P. reichenowi* (primate parasite group1) had 5– 6 SERA genes of Group IV by multiple gene duplications. In the lineage leading to three rodent parasites, a Group IV SERA gene was duplicated. In lineages of primate parasite group2 (*P. malariae*, *P. ovale*, and *P. vivax* and related monkey parasites), gene duplications of Group IV SERA gene took place in each parasite lineage resulting to 4 SERA genes in *P. ovale*, 7 SERA genes in *P. malariae* and 2–9 SERA genes in *P. vivax* and related monkey parasites. Simultaneously, gene deletions as well as pseudogenization and truncation also took place in Group IV SERA genes of *P. vivax* and related monkey parasites. It is notable that gene duplication events occurred only in Group IV SERA genes in mammalian parasites and this duplication was particularly frequent in parasite species that infect humans, apes and monkeys.

In general, duplicated genes undergo either (i) concerted evolution or (ii) birth-and-death evolution [2]. Homogenization of duplicated genes by gene conversion drives concerted evolution as evident in the rRNA multigene families of vertebrates; while duplicated genes show divergence by independent diversification processes to result in birth-and-death evolution, e.g., the major histocompatibility complex (MHC) gene families of mammals. The birth-and-death evolution model applies to most multigene families. The model assumes that new genes are created by

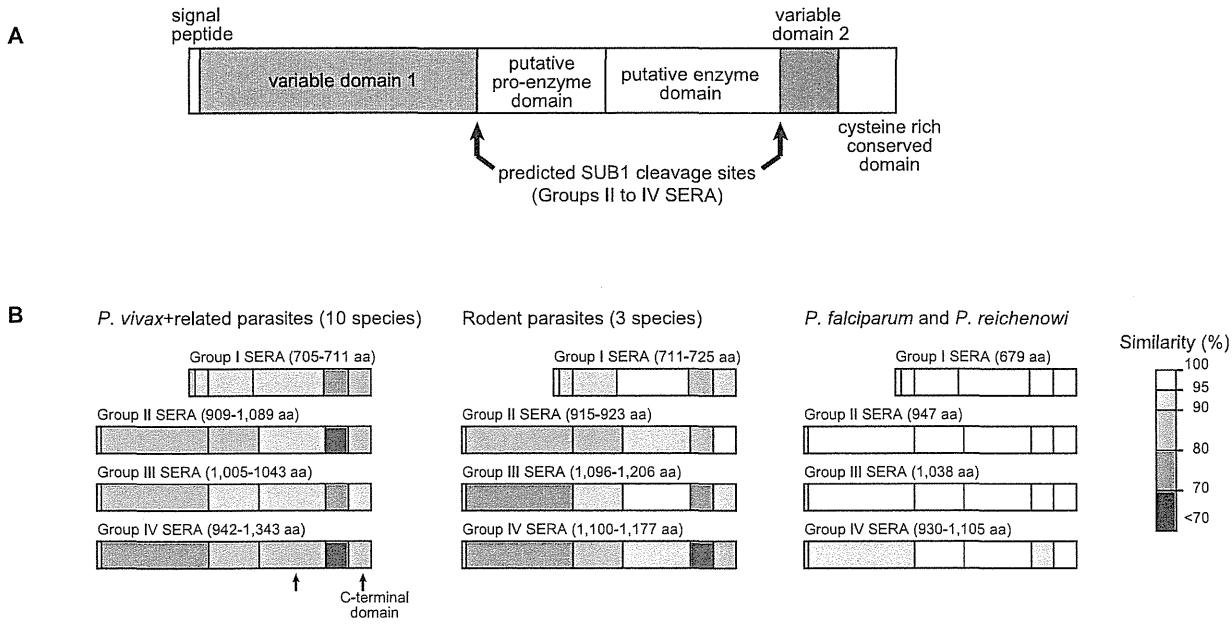

Figure 3. Primary structure and inter-species sequence variation of the *Plasmodium* SERA gene. The putative domain structure of the gene family is shown in (A). In (B) are sequence variations in Groups I to IV SERA domains using amino acid sequence similarity for three parasite lineages: (i) *P. vivax* and *P. vivax*-related monkey malaria parasite species, (ii) three rodent parasite species, and (iii) *P. falciparum* and *P. reichenowi*. Percent (%) similarity is color coded.
doi:10.1371/journal.pone.0017775.g003

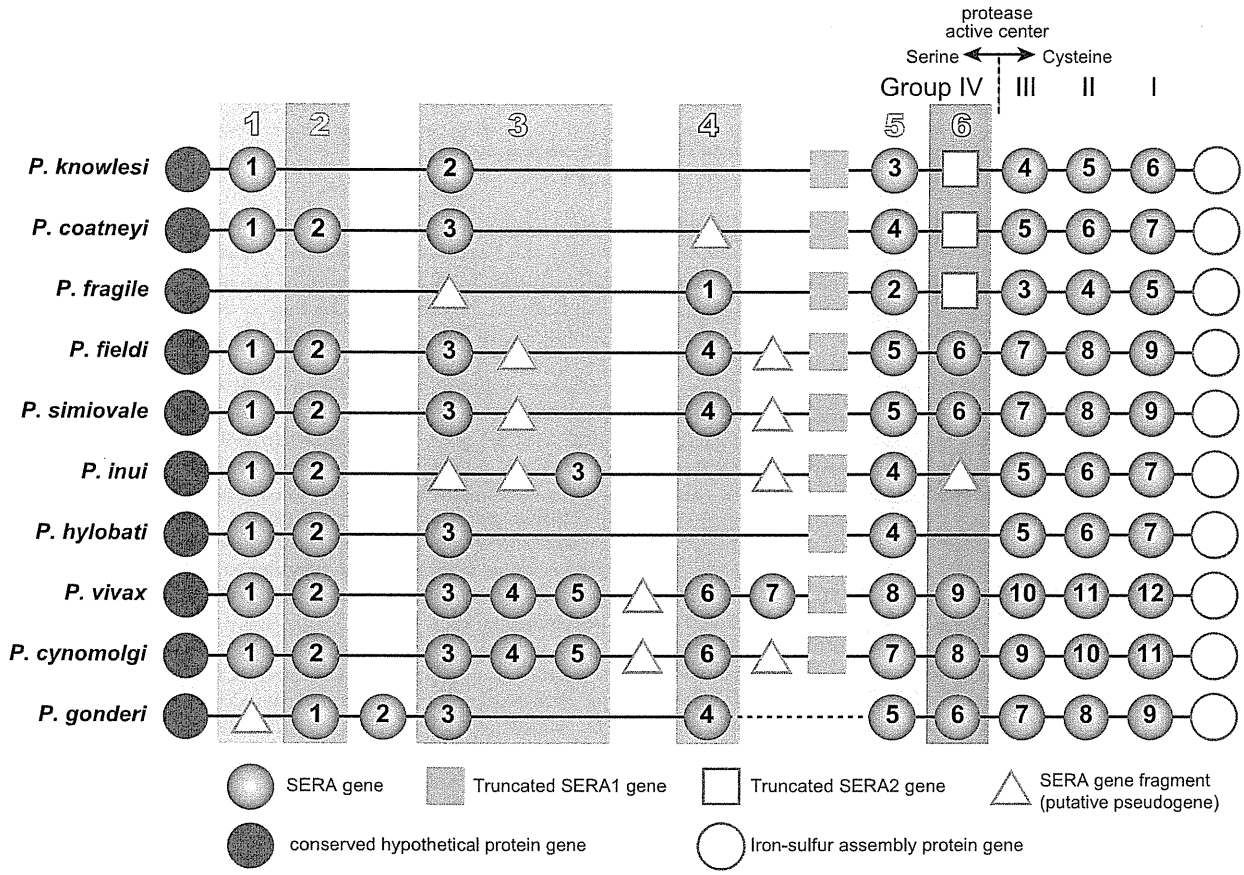

Figure 4. The SERA gene organization of *P. vivax* and *P. vivax*-related monkey malaria parasites. Six monophylic clades of Group IV SERA genes, Clade 1 to Clade 6 are designated in colored boxes. SERA genes, truncated SERA genes and SERA gene fragments are shown by light gray circle, square, and triangle, respectively. The conserved hypothetical protein gene at 5′-end and the iron-sulfur assembly protein gene at the 3′-end are shown by dark gray circle and open circle, respectively.
doi:10.1371/journal.pone.0017775.g004

repeated gene duplications; and that duplicated genes can be maintained in the genome for a long time, whereas others become deleted or nonfunctional through deleterious mutations [2]. The observed gene duplication and gene deletion found in the *Plasmodium* SERA genes is in concordance with the birth-and-death model, though traits of gene conversion are detected in a few Group IV SERA genes of limited parasites. The birth-and-death model also has been recently proposed for gene duplication/gene deletion of msp-7, an immune target parasite surface antigen gene [24]. It may thus be argued that diversification of *Plasmodium* SERA multigene family was, likewise, driven by the birth-and-death evolution.

It is worth noting that gene duplication/gene deletion of serine-type Group IV SERA genes occurred primarily in *P. vivax* and related monkey malaria parasites. The reason for this lineage-specific evolutionary event is presently unknown. We consider that the gene duplication/gene deletion may be associated with an expansion of host range during the radiation of macaques that took place about 4–5 million years ago in Asia [25]. *P. vivax* related monkey parasites generally infect multiple hosts. For example, *P. knowlesi* and *P. cynomolgi* have the ability to infect a wide variety of macaques and humans [26]. The exception is *P. vivax*, which became a human parasite by host switch [18,27]. It is likely that Asian macaque malaria parasites radiated along with radiation events of host monkey species [28]. Duplicated SERA genes might have gained a new pathway in the process of merozoite release or parasite egress from infected erythrocytes, and ancestral parasites that diversified duplicated SERA genes might have succeeded in expanding its host range during the radiation period. Alternatively, it can be assumed that duplicated SERA genes played an important role in immune evasion.

In *P. falciparum* and *P. berghei*, many SERA genes could be disrupted without any obvious phenotypic change and appear to be non-essential. If non-functional, the birth-and-death evolution model assumes that these genes could have been gradually deleted or become pseudogenes. But many *Plasmodium* SERA genes have sequence similarity with each other even in different species and, moreover, transcription and/or translation can be detected in the different family members. These observations suggest that some SERA gene family member may play a role in the parasite life cycle. Titers of anti-Pfa-SERA5 IgG antibodies show a strong negative correlation with malaria symptom [4]. Despite being an abundantly expressed antigen, however, epidemiological studies provide evidence for low sero-conversion in individuals residing in malaria endemic areas compared to another abundant malaria blood stage antigen, merozoite surface protein 1 [4]. This may reflect the parasites' use of other strategies to evade immune responses, and it is tempting to speculate that SERA genes may

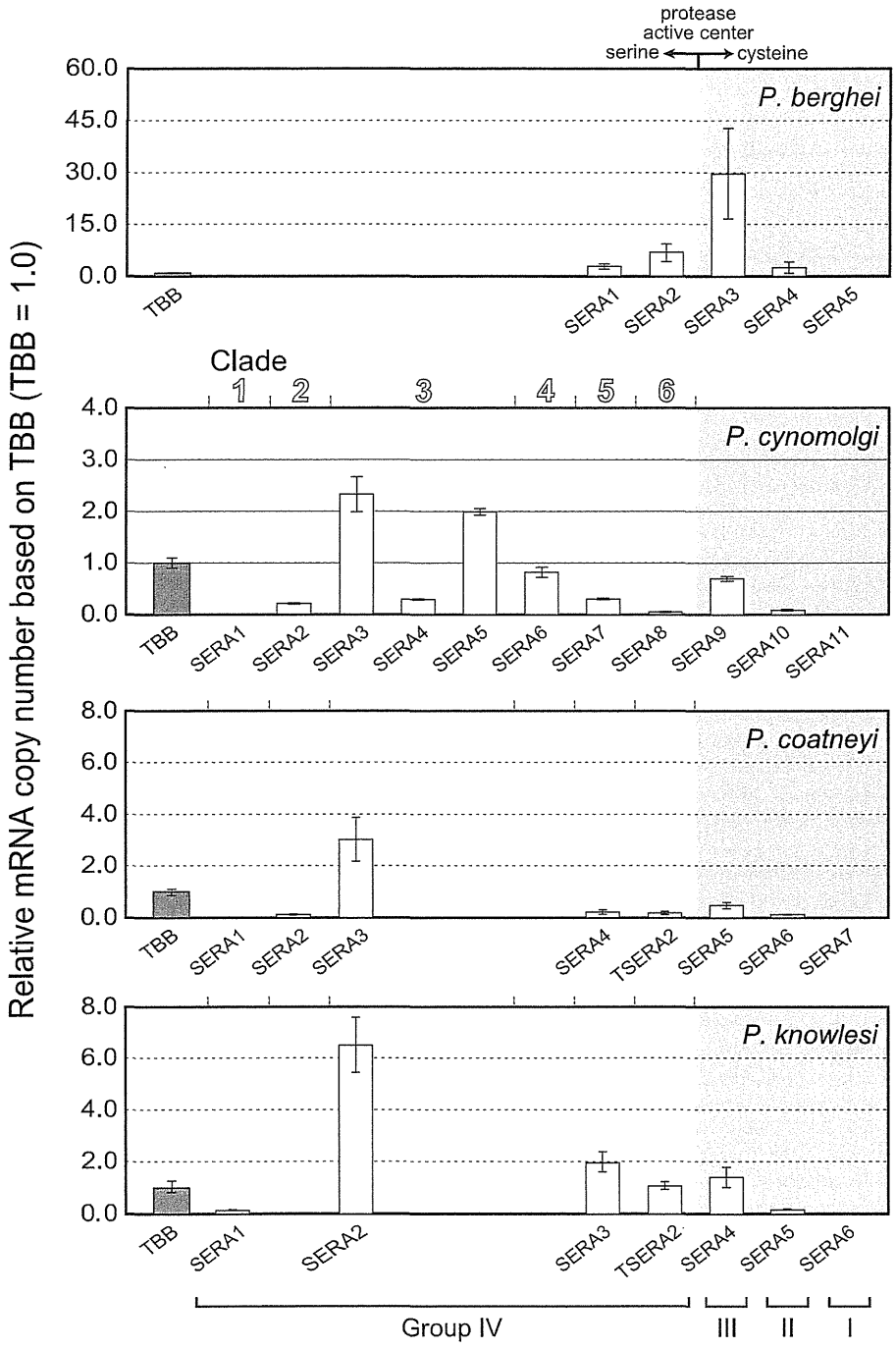

Figure 5. Transcription of the SERA gene family of rodent parasite *P. berghei*, and three monkey parasites, *P. cynomolgi*, *P. coatneyi* and *P. knowlesi*. Parasites at the late trophozoite to schizont stages were used for analyses. Relative amounts of transcribed SERA genes were standardized relative to β-tubulin (TBB), set at 1.0. Cysteine-type SERA genes (Groups I, II and III) and serine-type SERA genes (Group IV) are arrayed in gray shaded areas and unshaded areas, respectively. SERA genes of three monkey parasites are separated into six clades, as designated on top of the *P. cynomolgi* panel.
doi:10.1371/journal.pone.0017775.g005

play a role in this. It should be mentioned that SERA genes have inter-species variable sequence regions, variable domains 1 and 2, in which amino acid sequence variations are extensive including various tandem repeats. Sequence divergence would have been favorable for parasites to evade host immunity. Some ancestral parasites that gained diversified multiple SERA genes may have succeeded in adapting to newly appeared macaque species, thus leaving a signature for ancestral gene duplications. Gene

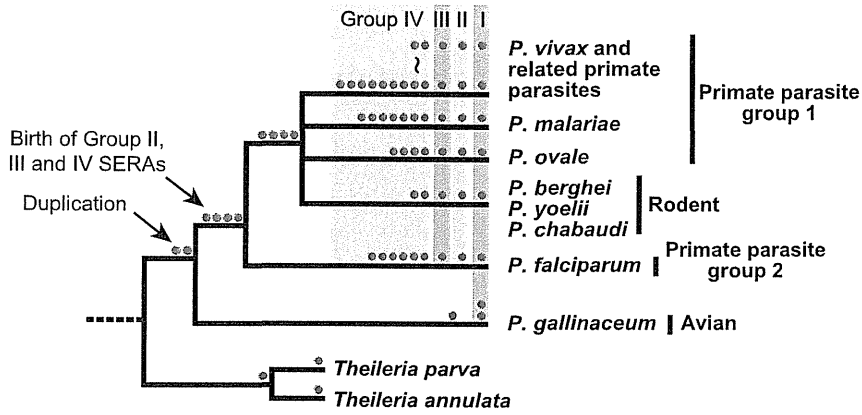

Figure 6. Inferred gene duplication events in the evolution of the *Plasmodium* SERA gene family. Each colored circle represents cysteine-type SERA gene (Groups I to III, green circle) and serine-type SERA genes (Group IV, blue circle), and is placed alongside parasite lineages of a generally accepted phylogenetic tree of *Plasmodium*, with *Theileria* used as an outgroup.
doi:10.1371/journal.pone.0017775.g006

duplication of Group IV SERA genes was also observed in *P. malariae*, *P. ovale* and *P. falciparum/P. reichenowi*. Recent findings of infections of these parasites as well as new parasite species in Great Apes (chimpanzees, bonobos and gorillas) indicate that these parasites show a wider host range than previously thought [29–35]. Investigations of SERA genes in newly identified Great Ape malaria parasites may reveal variation in the number of Group IV SERA genes. It is thus assumed that Group IV SERA genes of these parasites have also undergone the -and-death evolution. Together, birth-and-death evolution of Group IV SERA genes is likely to be common in primate parasites which have multiple hosts.

The present evolutionary and experimental (expression) analyses, when coupled with previous gene disruption studies using *P. falciparum* and *P. berghei*, shed some light on the importance of SERA proteins to malaria parasites. The presence of Group I SERA gene in all 18 *Plasmodium* species examined suggests that the gene is maintained by *Plasmodium* for its function. Disruption of *P. berghei* Group I SERA (Pbe-SERA5) blocked parasite development at the mosquito stage by inhibiting egress of sporozoites from an oocyst [36]. It is thus likely that Group I SERA gene encodes a protein involved in sporozoite egress for other parasite species; and therefore, not surprising to see no expression of Group I SERA genes at the blood stage of *P. berghei* and three *P. vivax*-related monkey parasites. Group II SERA gene is present in all *Plasmodium* species, except *P. gallinaceum*. This group is also expressed, as evident from the four parasites used for expression analysis and, likewise, from studies on Group II SERA genes of *P. falciparum* [7] and *P. vivax* [37]. These suggest the importance of this gene at the blood stage, although disruption of *P. falciparum* Pfa-SERA7 and *P. berghei* Pbe-SERA4 (Group II SERA genes) were nonlethal [38, Arisue et al. unpublished]. All 17 mammalian *Plasmodium* species have Group III SERA gene; and disruption of Group III SERA genes (Pfa-SERA6 and Pbe-SERA3) has been unsuccessful in both *P. falciparum* and *P. berghei* [38,39]. Pfa-SERA6 was suggested to be involved in schizont rupture and merozoite release from an infected erythrocyte [15]. Considerable expression of Pbe-SERA3 and Group III SERA genes in *P. vivax*-related monkey parasites suggests that Group III SERA gene is essential to all mammalian *Plasmodium* at the blood stage.

In contrast to Groups I to III, Group IV includes multiple SERA genes in all mammalian parasites. Contrary to clear orthologous relationship of Group I to III SERA genes, orthologous relationship in Group IV was not clearly seen across all mammalian parasites, although relationship was identified in mammalian parasite sub-groups (Figure 1). This suggests that the relative importance of individual SERA genes varies among parasite lineages. In the lineage of *P. falciparum* and *P. reichenowi*, most SERA genes of Group IV are orthologous. Pfa-SERA5 has been shown to be essential for parasite survival [40]. The importance of other Group IV SERA genes in this lineage cannot be ruled out because of substantial expression of these genes at the blood stage [7]. In the three rodent parasites, two Group IV SERA genes are orthologous. In *P. berghei*, simultaneous disruption of the two SERA genes does not affect parasite growth [39]; however, substantial expression of these two genes, as observed in this study, cannot rule out their importance in rodent parasites. In the lineage of *P. vivax* and related monkey parasites, Group IV SERA genes are further categorized into six clades. In Clade 5, all ten species have one SERA gene and in the *P. vivax* ortholog, Pvi-SERA8, expression has been detected [37]. All species but *P. fragile* have one to three SERA genes in Clade 3. Two *P. vivax* orthologs, Pvi-SERA4 and Pvi-SERA5 have been shown to be abundantly expressed [37]. Here we also observed high levels of transcription of Clade 3 SERA genes from three *P. vivax*-related monkey parasites (Pcy-SERA3 and 5, Pco-SERA3, and Pkn-SERA2). These suggest that SERA genes of Clade 3 and 5 likely play an important role at the blood stage. The substantial expression of SERA genes observed for other clades in the three monkey parasites as well as in *P. vivax* [37] suggests some role in each parasite species.

In conclusion, this study presents an overview of the evolution of the *Plasmodium* SERA gene family. The gene family was incipiently born in a common ancestor of the genus *Plasmodium*. Gene duplications during the parasite evolution generated two types of SERA genes, the cysteine-type SERA genes (Groups I to III) and the serine-type SERA genes (Group IV). Of note is that in mammalian malaria parasites, gene duplication occurred only in Group IV SERA genes, particularly frequent in primate parasites. Diversification of duplicated SERA genes supports the birth-and-death evolution in this gene family. It is intriguing to assume that duplications of SERA genes were associated with the parasite's expansion of host range. This study thus points to unique features of the *Plasmodium* SERA gene family and reinforces the importance of investigating other uncharacterized gene families of *Plasmodium*

to further understand the evolutionary history and biology of this parasite.

Materials and Methods

DNA sequences

DNA sequences of the *Plasmodium* SERA gene family were determined for the following eleven parasite species: *P. malariae*, *P. ovale*, *P. gonderi*, *P. fragile*, *P. coatneyi*, *P. knowlesi*, *P. inui*, *P. fieldi*, *P. simiovale*, *P. cynomolgi*, and *P. hylobati* (Table 1). For PCR amplification, we initially targeted conserved protease domains of SERA genes, and conserved regions from the conserved hypothetical protein (HP) gene and the putative iron-sulfur assembly protein gene (hesB) (Figure S5). Sets of degenerate primers were designed for each of the conserved protease regions (Table S1). For *P. knowlesi*, primers were designed using the parasite genome sequences [41]. The PCR products were cloned into a plasmid vector and sequenced (see below). Additional specific primers were designed based from sequenced regions for further amplification and confirmation of HP, SERA genes and hesB (Figure S5). More than five clones for each fragment were sequenced on both strands by primer walking. Finally, obtained sequences were verified by direct sequencing, using sequencing primers designed to cover target regions in both directions. Using this sequence strategy, we successfully obtained 116 SERA gene sequences located between the HP gene and hesB from all but one parasite species, *P. gonderi*. Despite extensive trials of amplifications, including several long-PCR protocols, for some unknown reasons, we failed to amplify a SERA family gene member between the region of Pgo-SERA4 and Pgo-SERA5 (Figure S5). This unamplified sequence may be a very long intergenic region lacking an SERA gene. The 3′ terminus of Pgo-SERA4 and the 5′ terminus of Pgo-SERA5 were, however, determined by amplification using the uneven PCR method [42]. Phusion DNA polymerase (Finnzymes) was used for PCR using degenerate primers. Pfu (Promega), and KOD-FX (TOYOBO) or LA-Taq (Takara) were used for amplification of fragments shorter than 2 kb or those longer than 2 kb, respectively. The PCR condition was 2 min at 94°C, followed by 40 cycles at 94°C for 15 sec, x°C for 30 sec and 68°C for y min, with final elongation of 5 min at 68°C. Annealing temperature, x, was set 2-3°C below the *Tm* of primers, which was calculated using Genetyx ver. 9 (GENETYX Co.). The extension time, y (min), was set at 1 min per 1 kb. Amplified fragments were cloned into pCR Blunt II TOPO vector or pCR XL TOPO vector (Invitrogen). Fragments amplified using KOD-FX were dA-tailed with A-attachment mix (TOYOBO) before TA-cloning. DNA sequencing was conducted on a 3130 Genetyx Analyzer (Applied Biosystems, Foster City, CA). SERA gene sequences reported in this study were deposited in DDBJ, with accession numbers AB576870-AB576881 (Table 1).

Sequence alignment

Analyses was done for 116 SERA genes obtained, together with 49 SERA sequences retrieved in public database from seven *Plasmodium* species: *P. falciparum*, *P. vivax*, *P. reichenowi*, *P. yoelii*, *P. berghei*, *P. chabaudi* and *P. gallinaceum* (Table S2). Open reading frame of each SERA gene was predicted by comparison to *P. falciparum*-SERA genes. A total of 134 predicted SERA amino acid sequences from 18 *Plasmodium* species were aligned using CLUSTAL W program under default options [43] with manual corrections. The sequence alignment obtained here and amino acid sites used in the present analyses are shown in Figure S2. Amino acid sequence similarity among orthologous SERA genes was calculated by the Nei and Gojobori method implemented in MEGA version 4 [44] using pairwise deletion option and overall average of p-distance is presented.

Phylogenetic analyses

Maximum likelihood (ML) trees were constructed using PROML programs in PHYLIP version 3.69 [45]. Jones-Taylor-Thornton (JTT) amino acid substitution model [46] was used. To take the evolutionary rate heterogeneity across sites into consideration, the R (Hidden Markov Model rates) option was set for discrete Γ distribution with 8 categories approximating the site-rate distribution. CODEML programs in PAML 4.4 [47,48] were used for estimating the Γ shape parameter, α values. For bootstrap analyses, SEQBOOT program in PHYLIP was applied to generate resampled datasets. Five hundred replicates were used for analyses. Bootstrap proportion values were calculated for internal branches of each tree using the CONSENSE program in PHYLIP.

Transcription analyses

Parasitized erythrocytes were obtained from mice infected with *P. berghei* (ANKA) and from Japanese macaques, *Macaca fuscata*, infected with *P. coatneyi* (CDC), *P. knowlesi* (H) or *P. cynomolgi* (B). Blood was taken several times with 4 to 12 hour intervals and parasites at the late trophozoite stage were selected for transcription analyses.

Studies using mice were approved by Animal Care and Use Committee of Gunma University and conducted in compliance with guidelines (Permit ID: 10-007). The experimental monkeys were second-generation offspring bred in captivity. The investigators adhered to the Guidelines for the Use of Experimental Animals authorized by the Japanese Association for Laboratory Animal Science. The protocol was approved by the Committee on Ethics of Animal Experiments at Dokkyo University School of Medicine (Permit Number: 0536). All procedures were performed under anesthesia by a combination of ketamine hydrochloride (10 mg/kg, i.m.) and xylaxine (0.5 mg/kg, i.m.), and all efforts were made to minimize suffering. The details of animal welfare/care and steps taken to ameliorate suffering were in accordance with the recommendations of the Weatherall report, "The use of non-human primates in research".

Total RNA was isolated by RNeasy Mini kit (QIAGEN) according to the manufacture's protocol. First strand cDNA was synthesized with Superscript III First-strand System for RT-PCR (Invitrogen) using 20 μg of total RNA. To confirm SERA gene transcriptions, PCR amplifications were performed using synthesized cDNA and specific primers for each SERA gene. Since no PCR product can be obtained for *P. cynomolgi*-SERA1 gene and *P. coatneyi*-SERA1 gene, these were excluded from further analysis.

Real time quantitative PCR was performed using ABI PRISM 7900 (Applied Biosystems), and results were analyzed with the SDS software version 2.2 (Applied Biosystems). A 15 ul mixture was formulated with 7.5 ul of TaqMan Gene Expression Master Mix (Applied Biosystems), an appropriate volume of first strand cDNA, 3 pmol of forward and reverse primers, and 0.5 pmol TaqMan probe. Sequences of primers and probes are shown in Table S3. The PCR condition was 2 min at 50°C and 10 min at 95°C, followed by 40 cycles at 95°C for 15 sec and 60°C for 1 min. Relative mRNA copy number of SERA genes within each species was compared using the internal control β-tubulin. Standard curves were generated using serially diluted cDNA template for each β-tubulin and SERA gene. After confirming the reproducible linearity of the curve where R° value is >0.98, threshold cycles (Ct) of each gene was applied to the curve and the relative expression amount of each SERA gene was calculated

against β-tubulin in each run. Experiments were conducted three times with triplicate samples.

Supporting Information

Figure S1 The SERA gene family drawn to scale in17 *Plasmodium* species. The 5′-end of each gene map is set at the start codon position of the conserved hypothetical protein gene, whose transcriptional direction is opposite to that of SERA genes. SERA genes of Groups I to III (cysteine-type) and those of Group IV (serine-type) are shown in green and blue, respectively. TSERA denotes truncated SERA genes shown in yellow. SERA gene fragments (putative pseudogenes) are in gray. The region that was not successfully sequenced in *P. gonderi* is indicated by a double slash [*P. reichenowi* SERA genes in this region are not shown due to the lack of complete sequences].
(EPS)

Figure S2 Amino acid sequence alignments of 134 *Plasmodium* SERA genes. Amino acid sites used for constructing phylogenetic trees for Figure 2 (570 amino acid sites) and Figure S3 (392 amino acid sites) are marked (#). The catalytic serine and cysteine residues are shaded in green and pink, respectively. Other active site residues are shaded in yellow. Tandem repeats of serine residues are highlighted in red. Putative PfSUB1 recognition motives are shaded in blue.
(DOC)

Figure S3 The maximun likelihood phylogenetic tree of the *Plasmodium* SERA gene family. This unrooted tree was constructed from 134 SERA genes using 392 amino acid sites under the JTT and Γ (8 catogories) model ($\alpha = 0.96$) with 500 heuristic replicates. Bootstrap values >50% are shown along nodes. Groups I-III and Group IV are cysteine-type and serine-type protease SERA genes, respectively.
(EPS)

Figure S4 Amino acid sequence alignments of Group IV Clade 6 SERA genes of *P. vivax* and *P. vivax*-related monkey malaria parasite species. The catalytic serine residue and other active site residues are shaded in green and yellow, respectively. Asterisks denote stop codons. Putative PfSUB1 recognition motifs are shaded in blue. The long deletion in truncated SERA genes of *P. coatneyi*, *P. knowlesi* and *P. fragile* are highlighted in black.
(DOC)

Figure S5 Sequencing strategy for the SERA gene family in 11 *Plasmodium* species. Thick bars indicate conserved protease domain of SERA genes targeted for PCR amplification and sequencing. Primer names are given in either ends of bars, and their sequences are listed in Table S1. The region that was not successfully sequenced in *P. gonderi* is shown by a double slash. SERA genes of Group I to III (cysteine-type SERA gene) and those of Group IV (serine-type SERA gene) are shown in green and blue, respectively. TSERA denotes truncated SERA gene shown in yellow. SERA gene fragments are shown in gray. In this study, the H strain of *P. knowlesi* (ATCC 30158) is different from the H strain used for the genome sequencing [41] for unknown reasons. The number of SERA genes and the organization of the SERA gene family, however, are identical between the two, and the sequence identity of SERA gene family region is 95.5%.
(EPS)

Table S1 PCR Primers used.
(PDF)

Table S2 SERA gene accession numbers in PlasmoDB database.
(PDF)

Table S3 Primers and probes used for real time PCR.
(PDF)

Acknowledgments

The authors thank Dr Richard Culleton (Nagasaki University, Japan) for providing us genomic DNA of *P. ovale* (Nigeria II strain), Dr. Ananias A. Escalante for providing us genomic DNAs of *P. inui* (Celebes strain) and *P. fragile* (Hackeri strain). Sequence analyses were supported by Central Instrumentation Laboratory, transcription analyses were supported by DNA-chip Development Center for Infectious Diseases, and phylogenetic analyses were done by using the computing system in Genome Information Research Center, Research Institute for Microbial Diseases, Osaka University.

Author Contributions

Conceived and designed the experiments: NA KT TH. Performed the experiments: NA SK MH NMQP MJ AK. Analyzed the data: NA KT. Wrote the paper: NA NMQP SK MH KT TH. Obtained permission for animal use: SK MH.

References

1. Janssen CS, Phillips RS, Turner CM, Barrett MP (2004) *Plasmodium* interspersed repeats: the major multigene superfamily of malaria parasites. Nucleic Acids Res 32: 5712–5720.
2. Nei M, Rooney AP (2005) Concerted and birth-and death evolution of multigene families. Annu Rev Genet 39: 121–152.
3. Gardner MJ, Hall N, Fung E, White O, Berriman M, et al. (2002) Genome sequence of the human malaria parasite *Plasmodium falciparum*. Nature 419: 498–511.
4. Horii T, Shirai H, Jie L, Ishii KJ, Palacpac NQ, et al. (2010) Evidences of protection against blood-stage infection of *Plasmodium falciparum* by the novel protein vaccine SE36. Parasitol Int 593: 380–386.
5. Okech BA, Nalunkuma A, Okello D, Pang XL, Suzue K, et al. (2001) Natural human immunoglobulin G subclass responses to *Plasmodium falciparum* serine repeat antigen in Uganda. Am J Trop Med Hyg 65: 912–917.
6. Okech B, Mujuzi G, Ogwal A, Shirai H, Horii T, et al. (2006) High titers of IgG antibodies against *Plasmodium falciparum* serine repeat antigen 5 (SERA5) are associated with protection against severe malaria in Ugandan children. Am J Trop Med Hyg 74: 191–197.
7. Aoki S, Li J, Itagaki S, Okech BA, Egwang TG, et al. (2002) Serine repeat antigen (SERA5) is predominantly expressed among the SERA multigene family of *Plasmodium falciparum*, and the acquired antibody titers correlate with serum inhibition of the parasite growth. J Biol Chem 277: 47533–47540.
8. Inselburg J, Bathurst IC, Kansopon J, Barchfeld GL, Barr PJ, et al. (1993) Protective immunity induced in Aotus monkeys by a recombinant SERA protein of *Plasmodium falciparum*: adjuvant effects on induction of protective immunity. Infect Immun 61: 2041–2047.
9. Inselburg J, Bathurst IC, Kansopon J, Barr PJ, Rossan R (1993) Protective immunity induced in Aotus monkeys by a recombinant SERA protein of *Plasmodium falciparum*: further studies using SERA 1 and MF75.2 adjuvant. Infect Immun 61: 2048–2052.
10. Sugiyama T, Suzue K, Okamoto M, Inselburg J, Tai K, et al. (1996) Production of recombinant SERA proteins of *Plasmodium falciparum* in *Escherichia coli* by using synthetic genes Vaccine 14: 1069–1076.
11. Delplace P, Fortier B, Tronchin G, Dubremetz JF, Vernes A (1987) Localization, biosynthesis, processing and isolation of a major 126 kDa antigen of the parasitophorous vacuole of *Plasmodium falciparum*. Mol Biochem Parasitol 23: 193–201.
12. Debrabant A, Maes P, Delplace P, Dubremetz JF, Tartar A, et al. (1992) Intramolecular mapping of *Plasmodium falciparum* P126 proteolytic fragments by N-terminal amino acid sequencing. Mol Biochem Parasitol 53: 89–95.
13. Li J, Matsuoka H, Mitamura T, Horii T (2002) Characterization of proteases involved in the processing of *Plasmodium falciparum* serine repeat antigen (SERA) Mol Biochem Parasitol 120: 177–186.
14. Li J, Mitamura T, Fox BA, Bzik DJ, Horii T (2002) Differential localization of processed fragments of *Plasmodium falciparum* serine repeat antigen and further processing of its N-terminal 47 kDa fragment. Parasitol Int 51: 343–352.

15. Yeoh S, O'Donnell RA, Koussis K, Dluzewski AR, Ansell KH, et al. (2007) Subcellular discharge of a serine protease mediates release of invasive malaria parasites from host erythrocytes. Cell 131: 1072–1083.
16. Arastu-Kapur S, Ponder EL, Fonovic UP, Yeoh S, Yuan F, et al. (2008) Identificartion of proteases that regulate erythrocyte rupture by the malaria parasite *Plasmodium falciparum*. Nat Chem Biol 4: 203–210.
17. Arisue N, Hirai M, Arai M, Matsuoka H, Horii T (2007) Phylogeny and evolution of the SERA multigene family in the genus *Plasmodium*. J Mol Evol 65: 82–91.
18. Escalante AA, Cornejo OE, Freeland DE, Poe AC, Durrego E, et al. (2005) A monkey's tale: the origin of *Plasmodium vivax* as a human malaria parasite. Proc Natl Acad Sci USA 102: 1980–1985.
19. Hayakawa T, Culleton R, Otani H, Horii T, Tanabe K (2008) Big bang in the evolution of extant malaria parasites. Mol Biol Evol 25: 2233–2239.
20. Ricklefs RE, Outlaw DC (2010) A molecular clock for malaria parasites. Science 329: 226–229.
21. Bzik DJ, Li WB, Horii T, Inselburg J (1988) Amino acid sequence of the serine-repeat antigen (SERA) of *Plasmodium falciparum* determined from cloned cDNA. Mol Biochem Parasitol 30: 279–288.
22. Hodder AN, Drew DR, Epa VC, Delorenzi M, Bourgon R, et al. (2003) Enzymic, phylogenetic, and structural characterization of the unusual papain-like protease domain of Plasmodium falciparum SERA5. J Biol Chem 278: 48169–48177.
23. Hodder AN, Malby RL, Clarke OB, Fairlie WD, Colman PM, et al. (2009) Structural insights into the protease-like antigen *Plasmodium falciparum* SERA5 and its noncanonical active-site serine. J Mol Biol 392: 154–65.
24. Garzón-Ospina D, Cadavid LF, Patarroyo MA (2010) Differential expansion of the merozoite surface protein (msp)-7 gene family in *Plasmodium* species under a birth-and-death model of evolution. Mol Phylogenet Evol 55: 399–408.
25. Ziegler T, Abegg C, Meijaard E, Perwitasari-Farajallah D, Walter L, et al. (2007) Molecular phylogeny and evolutionary history of Southeast Asian macaques forming the M. silenus group. Mol Phylogenet Evol 42: 807–816.
26. Coatney GR, Collins WE, Warren M, Contacos PG (1971) The Primate Malarias. Washington DC: US Government Printing Office.
27. Mu J, Joy DA, Duan J, Huang Y, Carlton J, et al. (2005) Host switch leads to emergence of *Plasmodium vivax* malaria in humans. Mol Biol Evol 22: 1686–1693.
28. Fooden J (1994) Malaria in Macaques. Int J Primatol 15: 573–596.
29. Hayakawa T, Arisue N, Udono T, Hirai H, Sattabongkot J, et al. (2009) Identification of *Plasmodium malariae*, a human malaria parasite, in imported chimpanzees. PLoS One 4: e7412.
30. Duval L, Nerrienet E, Rousset D, Sadeuh Mba SA, Houze S, et al. (2009) Chimpanzee malaria parasites related to *Plasmodium ovale* in Africa. PLoS One 4: e5520.
31. Ollomo B, Durand P, Prugnolle F, Douzery E, Arnathau C, et al. (2009) A new malaria agent in African hominids. PLoS Pathog 5: e1000446.
32. Krief S, Escalante AA, Pacheco MA, Mugisha L, André C, et al. (2010) On the diversity of malaria parasites in African apes and the origin of *Plasmodium falciparum* from Bonobos. PLos Pathog 6: e1000765.
33. Prugnolle F, Durand P, Neel C, Ollomo B, Ayala FJ, et al. (2010) African great apes are natural hosts of multiple related malaria species, including *Plasmodium falciparum*. Proc Natl Acad Sci USA 107: 1458–1463.
34. Duval L, Fourment M, Nerrienet E, Rousset D, Sadeuh SA, et al. (2010) African apes as reservoirs of *Plasmodium falciparum* and the origin and diversification of the *Laverania subgenus*. Proc Natl Acad Sci USA 107: 10561–10566.
35. Liu W, Li Y, Learn GH, Rudicell RS, Robertson JD, et al. (2010) Origin of the human malaria parasite *Plasmodium falciparum* in gorillas. Nature 467: 420–425.
36. Aly ASI, Matuschewski K (2005) A malarial cysteine protease is necessary for *Plasmodium* sporozoite egress from oocysts. J Exp Med 202: 225–230.
37. Palacpac NM, Leung BW, Arisue N, Tanabe K, Sattabongkot J, et al. (2006) *Plasmodium vivax* serine repeat antigen (SERA) multigene family exhibits similar expression patterns in independent infections. Mol Biochem Parasitol 150: 353–358.
38. Miller SK, Good RT, Drew DR, Delorenzi M, Sanders PR, et al. (2002) A subset of *Plasmodium falciparum* SERA genes are expressed and appear to play an important role in the erythrocytic cycle. J Biol Chem 277: 47524–47532.
39. Putrianti ED, Schmidt-Christensen A, Arnold I, Heussler VT, Matuschewski K, et al. (2010) The *Plasmodium* serine-type SERA proteases display distinct expression patterns and non-essential in vivo roles during life cycle progression of the malaria parasite. Cell Microbiol 12: 725–739.
40. McCoubrie JE, Miller SK, Sargeant T, Good RT, Hodder AN, et al. (2007) Evidence for a common role for the serine-type *Plasmodium falciparum* serine repeat antigen proteases: Implications for vaccine and drug design. Infect Immun 75: 5565–5574.
41. Pain A, Bohme U, Berry AE, Mungall K, Finn RD, et al. (2008) The genome of the simian and human malaria parasite *Plasmodium knowlesi*. Nature 455: 799–803.
42. Chen X, Wu R (1997) Direct amplification of unknown genes and fragments by Uneven polymerase chain reaction. Gene 185: 195–199.
43. Thompson JD, Higgins DG, Gibson TJ (1994) CLUSTAL W: improving the sensitivity of progressive multiple sequence alignment through sequence weighting, position-specific gap penalties and weight matrix choice. Nucleic Acids Res 22: 4673–4680.
44. Tamura K, Dudley J, Nei M, Kumar S (2007) *MEGA4*: Molecular Evolutionary Genetics Analysis (MEGA) software version 4.0. Mol Biol Evol 24: 1596–1599.
45. Felsenstein J (1996) Inferring phylogenies from protein sequences by parsimony, distance, and likelihood methods. Methods Enzymol 266: 418–427.
46. Jones DT, Taylor WR, Thornton JM (1992) The rapid generation of mutation data matrices from protein sequences. Comput Appl Biosci 8: 275–282.
47. Yang Z (1997) PAML: a program package for phylogenetic analysis by maximum likelihood. Comput Appl Biosci 13: 555–556.
48. Yang Z (2007) PAML 4: a program package for phylogenetic analysis by maximum likelihood. Mol Biol Evol 24: 1586–1591.

J. Biochem. 2012;152(3):259–268 doi:10.1093/jb/mvs058

JB THE JOURNAL OF BIOCHEMISTRY

Critical roles of the mitochondrial complex II in oocyst formation of rodent malaria parasite *Plasmodium berghei*

Received May 1, 2012; accepted May 16, 2012; published online May 23, 2012

Akina Hino[1,*], Makoto Hirai[2,3,*†], Takeshi Q. Tanaka[1,‡], Yoh-ichi Watanabe[1], Hiroyuki Matsuoka[3] and Kiyoshi Kita[1,§]

[1]Department of Biomedical Chemistry, Graduate School of Medicine, The University of Tokyo, 7-3-1 Hongo, Bunkyo-ku, Tokyo 113-0033, Japan; [2]Department of Parasitology, Graduate School of Medicine, Gunma University, 3-39-22 Maebashi City, Gunma 371-8511, Japan and [3]Division of Medical Zoology, Department of Infection and Immunity, School of Medicine, Jichi Medical University, Shimotsuke City, Tochigi 329-0498, Japan

*These authors contributed equally to this study.

†Makoto Hirai, Department of Parasitology, Graduate School of Medicine, Gunma University, 3-39-22 Maebashi City, Gunma 371-8511, Japan. Tel: +81-27-220-8023, Fax: +81-27-220-8025, email: makotohirai@gunma-u.ac.jp

‡Present address: Laboratory of Malaria and Vector Research, National Institute of Allergy and Infectious Diseases, National Institutes of Health, Rockville, MD 20892, USA.

§Kiyoshi Kita, Department of Biomedical Chemistry, Graduate School of Medicine, The University of Tokyo, 7-3-1 Hongo, Bunkyo-ku, Tokyo 113-0033, Japan. Tel: +81-3-5841-3528, Fax: +81-3-5841-3444, email: kitak@m.u-tokyo.ac.jp

It is generally accepted that the mitochondria play central roles in energy production of most eukaryotes. In contrast, it has been thought that *Plasmodium* spp., the causative agent of malaria, rely mainly on cytosolic glycolysis but not mitochondrial oxidative phosphorylation for energy production during blood stages. However, *Plasmodium* spp. possesses all genes necessary for the tricarboxylic acid (TCA) cycle and most of the genes for electron transport chain (ETC) enzymes. Therefore, it remains elusive whether oxidative phosphorylation is essential for the parasite survival. To elucidate the role of TCA metabolism and ETC in malaria parasites, we deleted the gene for flavoprotein (Fp) subunit, *Pbsdha*, one of four components of complex II, a catalytic subunit for succinate dehydrogenase activity. The Pbsdha(-) parasite grew normally at blood stages in mouse. In contrast, ookinete formation of Pbsdha(-) parasites in the mosquito stage was severely impaired. Finally, Pbsdha(-) ookinetes failed in oocyst formation, leading to complete malaria transmission blockade. These results suggest that malaria parasite may switch the energy metabolism from glycolysis to oxidative phosphorylation to adapt to the insect vector where glucose is not readily available for ATP production.

Keywords: complex II/malaria parasite/mitochondria/*Plasmodium berghei*.

Abbreviations: AP, alkaline phosphatase; BCIP, 5-bromo-4-chloro-3'-indolylphosphatase *p*-toluidine salt; Cyt *b*, cytochrome *b*; Cyt *c*, cytchrome *c*; DHOD, dihydroorotate dehydrogenase; ETC, electron transport chain; FAD, flavin adenine dinucleotide; FBS, fetal bovine serum; Fp, flavoprotein; FRD, fumarate reductase; HRP, horse radish peroxidase; Ip, iron–sulphur cluster protein; MQO, malate–quinone oxidoreductase; MV, methylviologen; NAD, nicotineamide adenine dinucleotide; NBT, nitroblue tetrazolium chloride; NDH2, type2 NADH–ubiquinone oxidoreductase; Q, quinine; QFR, quinol–fumarate reductase; SDH, succinate dehydrogenase; SQR, succinate–ubiquinone reductase; TBS, tris buffered saline; TCA, tricarboxylic acid.

Malaria is one of the most serious diseases in the world. It causes one million infant deaths and over 500 million clinical cases annually, of which 85% is in sub-Saharan Africa (*1*). The drugs such as pyrimethamine/sulphadoxine, chloroquine or artesunate are the common treatment against malaria, but there is the emergence and spread of drug-resistant malaria parasites throughout the world (*2*), resulting in an urgent need for new drug.

The mitochondrion of *Plasmodium* species is obvious target of antimalarial drugs, but the physiological importance of this organelle is poorly understood. In other eukaryotes, pyruvate dehydrogenase is localized in mitochondria where it links the glycolysis metabolic pathway to TCA cycle, while it is localized in the apicoplast in *P. falciparum* (*3*). Therefore, it has been unclear until recently how glycolysis metabolism is connected to the tricarboxylic acid (TCA) cycle. Blood-stage *P. falciparum* have only a single mitochondrion without crista (*4*). Such morphologically immature mitochondrion suggests that, unlike other eukaryotes, the blood stage *P. falciparum* relies mainly on cytoplasmic glycolysis for their energy metabolism but not on mitochondrial oxidative phosphorylation (*5*, *6*). Beside, recent omics-based studies showed that *P. falciparum* expressed all TCA cycle enzyme genes and most ones for the electron transport chain (ETC), and that *P. falciparum* produced the intermediates of the TCA cycle (*7*). Moreover, the genes for TCA cycle are upregulated at mosquito stages (*8*). The gametocytes, precursor cells of gametes possess mitochondria with cristae (*9*). These data suggest that mitochondrial energy metabolism may have more crucial roles in insect stages than blood stages,

which have not been intensively investigated until recently.

The mitochondrial complex II (succinate–ubiquinone reductase: SQR) oxidizes succinate to produce fumarate as a TCA cycle member enzyme. In the anaerobic electron transfer system, complex II carries out fumarate reduction using quinol as an electron donor (quinol–fumarate reductase; QFR), which is the reverse reaction of SQR. Complex II consists of four subunits, flavoprotein (Fp), iron–sulphur cluster protein (Ip) and two small membrane anchor subunits, cytochrome *b* large (CybL) and small (CybS) subunits. The Fp with molecular mass of 70 kDa has a flavin adenine dinucleotide (FAD) covalently bound to a highly conserved histidine (His) residue. Fp and Ip form catalytic portion of the complex and this portion acts as a succinate dehydrogenase (SDH), catalyzing the oxidation of succinate by water-soluble electron acceptors such as phenazine methosulphate in SQR, while it acts as a fumarate reductase (FRD), catalyzing electron transfer from water-soluble electron donors such as reduced methylviologen (MV) to fumarate in QFR. FAD in the Fp receives the reducing equivalents from succinate and then transfers it to quinone by SQR activity where the two small membrane anchor subunits are indispensable (*10*). Thus, complex II functions as a link between the TCA cycle and the ETC, directly. While complex II has such critical roles in energy metabolisms, and Fp and Ip subunits genes are substantially conserved in various organisms (*3*, *11*), two small membrane anchor subunit genes are diverse and had not been detected in the genomes of *Plasmodium* spp., suggesting that plasmodial complex II is nonfunctional. However, recently our intensive database mining has identified putative plasmodial anchor subunit genes (*12*). Moreover, biochemical studies revealed that SQR activity of complex II was detected in the mitochondrial fraction of *P. yoelii* and *P. falciparum*, and the activity was inhibited by the ubiquinone-binding site inhibitor, atopenin A5 (*13–15*).

In this work, we took genetic approach to understand the physiological role of the parasite complex II using *P. berghei* as a model because the whole parasite life cycle can be monitored using mosquito and mouse as hosts. We generated transgenic *P. berghei* (Pbsdha(-)) in which the Fp subunit gene (*Pbsdha*) of complex II was deleted to inactivate complex II activities. By infecting mice and mosquitoes with the Pbsdha(-) parasites, we followed phenotype of the Pbsdha(-) parasite during the whole life cycle and found that complex II is essential for oocyst formation in the mosquito.

Materials and Methods

Maintenance of mosquitoes and parasites

Anopheles stephensi (SDA 500 strain) and *P. berghei* (ANKA clone 2.34) were maintained as described previously (*16*). *P. berghei*-infected mosquitoes were fed on naïve mice (Balb/c), and the resulting infected mice were referred to as passage 0 (P0). The P0 blood was injected intraperitoneally to the naïve mice and the passage one (P1) mice were used in the experiments. The experiments using animals and recombinant DNA were performed under the guidelines of the committee in Jichi University, and assigned permission no. is 08-14.

Generation of Pbsdha::AGFP parasites

The two fragments covering the 5'UTR and the first 60 amino acids (−3229 to +180 bp), and 3' UTR (1025 bp) of *Pbsdha* gene (PBANKA_051820) were amplified with primer pairs 5'UTRB4F/5'UTRB1R and 3'UTRB2F/3'UTRB3R, and *P. berghei* genomic DNA as template. The *Azami Green Fluorescent Protein* gene (*AGFP*) was amplified with the primers AzamiB1F/AzamiB2R. Each PCR fragment was cloned into *pDONRP4-P1R*, *P1-P2R* and *P2-P3R* vectors by BP clonase reaction (Invitrogen) to generate entry vectors (*5UTR/P4P1*, *AGFP/P1P2* and *3UTR/P2P3*). An R4-R3 fragment (Invitrogen) was inserted into *HindIII* site of *pBS-DHFR* vector (*17*) to generate an acceptor plasmid (*R4R3/pBS-DHFR*). The inserts of entry vectors were transferred to the acceptor plasmid by LR reaction using the Multisite Gateway Three-Fragment Vector Construction Kit (Invitrogen). In the final plasmid (*Pbsdha::AGFP*), 5' UTR and the first 60 amino acids of *Pbsdha* were fused to the *AGFP* gene. Thus, the expression of the *AGFP* reporter gene is under the control of the *Pbsdha* gene promoter. For parasite transfection, the plasmid was digested by *BstXI*, and the linearized plasmid was integrated into the parasite genome by single crossover homologous recombination. The parasite transfection and subsequent cloning were performed as described elsewhere (*18*). Correct integration events in Pbsdha::AGFP parasites clones were confirmed by Southern blot as described later in the text. The genomic DNA (10 μg) of Wild Type (WT) and Pbsdha::AGFP parasites was digested with *PacI* and *HpaI*, separated by 0.8% (w/v) agarose gel and transferred to the Hybond-N+ membrane (GE healthcare). PCR fragment (F1-HindIII/R1-HindIII) was labeled with AlkPhos Direct Labeling Reagent Kit (GE Healthcare) and used as probe for hybridization. The hybridization and washing were performed by following the manufacturer's protocol.

The expression of the AGFP gene at each developmental stage in Pbsdha::AGFP parasites was investigated as follows. To prepare the parasites at blood stages, the mouse blood (1 ml) infected with Pbsdha::AGFP parasites was collected, mixed with 120 ml RPMI1640 containing 25% fetal bovine serum (FBS) and cultured at 37°C for 16 hr by the candle-jar method (*19*). The parasites synchronized to schizonts were partially purified by Nycoprep 1.077 (*18*) and injected intravenously into mice tail veins. At 4 hr and 33 hr after injection, the parasites were synchronized to ring and trophozoite stages, respectively. A drop of tail blood was collected at these time points, and the AGFP signal in rings, trophozoites, and *in vitro* cultured schizonts was observed. For the analysis of AGFP expression in mosquito-stage parasites, the ookinetes were prepared *in vitro* as described in 'Examination of Pbsdha(-) parasite development'. The mosquitoes were fed on mice carrying Pbsdha::AGFP parasites and dissected on day 14 and 16 after the feeding. The AGFP signal in the oocysts (on midguts) and sporozoites (in salivary glands) as well as *in vitro*-cultured ookinetes was observed. The parasite was stained with 10 nM of MitoTracker Orange CMTM Ros (Molecular Probes) and DAPI (4',6-diamino-2-phenylindole) (Dako) to label mitochondria and nuclei, respectively. The fluorescent signal of MitoTracker, DAPI and AGFP was detected at 540 nm, 452 nm and 520 nm, respectively.

Targeted disruption of the Pbsdha gene

Two regions of the *Pbsdha* gene were amplified by PCR using primer pairs F1-HindIII/R1-HindIII and F2-EcoRI/R2-BamHI, and *P. berghei* genomic DNA as template. The PCR fragments were digested with respective restriction enzymes and cloned to *pBS-DHFR* to give a targeting plasmid, *pPbsdha(-)*. The *pPbsdha(-)* plasmid was digested with *ClaI* and *BamHI*, and the plasmid was introduced in *P. berghei* by electroporation. The correct recombination event of the clones was confirmed by diagnostic PCR using two primer sets, K1 (K1-F and R) and K2 (K2-F and R). Correct integration was also checked by Southern blot analysis as described earlier in the text. The genomic DNA of WT and Pbsdha(-) parasites was digested with *PacI*, and a PCR fragment (F1-HindIII/R1-HindIII) was used as probe. The contamination of WT parasites in Pbsdha(-) parasite clone was checked by PCR with primer set W (W-F and R). Two clones from two independent transfection experiments were isolated and analyzed further. All primer sequences are described in supplementary information.

Western blot analysis of mitochondrial fraction

The mitochondrial fractions were prepared from mouse leucocytes, *in vitro* cultured *P. falciparum*, and WT and Pbsdha(-) of *P. berghei* by N_2 cavitation methods (*13*, *14*). The mitochondrial fractions of mouse liver (10 μg/lane), WT and Pbsdha(-) of *P. berghei* (20 μg/lane) and *P. falciparum* (10 μg/lane) were loaded onto 10% SDS polyacrylamide gel electrophoresis and transferred to a nitrocellulose membrane (Whatman). The membrane was blocked with SuperBlock (Pierce) and washed with TBS-T (150 mM NaCl, 0.05% (v/v) Tween 20, 10 mM Tris-HCl; pH 7.5). To detect the Fp subunit, the membrane was hybridized with antiserum against the *P. falciparum* Fp peptide (*20*) as primary antibody (1/1,000 dilution) and alkaline phosphatase (AP) conjugated anti-rabbit IgG antiserum as secondary antibody (1/10,000 dilution). The AP enzyme activity on the membrane was visualized by a chromogenic method using NBT and BCIP. To confirm the equal loading of the samples on the gel, *P. berghei* heat shock protein 70 (HSP70) was used as internal control. The same membrane used in Fp detection was rehybridized with anti-HSP70 antiserum as primary antibody (1/100 dilution) and horse radish peroxidase (HRP) conjugated anti-mouse IgG antiserum as secondary antibody (1/10,000 dilution). HRP enzyme activity was detected as chemiluminescent signal by the Immobilon Western Chemiluminescent HRP Substrate (Millipore).

Measurement of SQR activity in mitochondrial fraction

The SQR enzyme activity assay was performed at 25°C with a V-660 spectrophotometer (JASCO, Tokyo, Japan). The enzyme activity of SQR was determined as quinone-mediated succinate: 2,4-dichlorophenolindophonol (DCIP) reductase in 30 mM Tris-HCl (pH 8.0) containing 10 mM potassium succinate, 100 μM ubiquinone-2 and 45 μM DCIP ($\varepsilon^{600nm} = 21\,mM^{-1}cm^{-1}$) in the presence of 2 mM KCN and 0.1 μM Atpenin A5 (Alexis Biochemicals). Atpenin A5 was proven to be a novel inhibitor specific to mouse leukocytes but not parasitic SQR activity at this concentration in our previous study (*13*).

Examination of Pbsdha(-) parasite development

To assess the growth rate of the parasites in mice, the red blood cells (RBC) (10^4) infected with either WT or Pbsdha(-) parasites were intravenously injected into tail vein of each of the four naïve mice. Subsequently, the tail blood was taken every 24 hr and the number of infected RBCs was counted. To investigate the male gametogenesis, the infected blood (10 μl) was added to 1 ml of fertilization medium (10 % (v/v) FBS in RPMI1640 (pH 8.2)) at 21°C. The sample (10 μl) was taken at 15 min and the number of exflagellating male gametes was counted. The rest of the sample was further incubated for 16 hr and the number of ookinetes was counted. The fertilization rate was calculated by the conversion rate of female gametocytes into ookinetes.

Infectivity of Pbsdha(-) parasite to mosquito and transmission to mouse

The tail blood of WT- and Pbsdha(-)-infected mice was taken and the number of exflagellating male gametes was counted. Only the mice whose blood contained over 2 exflagellating centers per 10^4 RBC were used for the mosquito feeding. Female mosquitoes (4–7 days old) were fed on the infected mice, and fully engorged mosquitoes were collected. Sixteen days after blood feeding, midguts and salivary glands were isolated. The number of oocysts in the midgut was counted and the presence of sporozoites in the salivary gland was examined to assess the infectivity of the parasites to mosquitoes. To investigate the transmission efficiency to mice, more than 20 mosquitoes carrying WT or Pbsdha(-) parasites were fed on naïve mice. The transmission of the parasites to mice was examined by checking mouse blood smears until 2 weeks after the mosquito feeding.

Results

Identification and expression analysis of Pbsdha

We found PBANKA_051820 being annotated as a putative Fp subunit gene of complex II in PlasmoDB, and hereafter it is referred to '*Pbsdha*'. It is known that amino acid sequences of Fp are highly conserved among various organisms. As such, the amino acid sequence of *P. berghei* FP (PbFp) shows high identity to those of other organisms including *P. falciparum* Fp, which we have reported previously (*11*). Especially, histidine in the FAD binding site in the catalytic domain is completely conserved in PbFp (Fig. 1).

To investigate *Pbsdha* gene expression during parasite life cycle, we generated Pbsdha::AGFP parasites as a reporter line, in which *AGFP* reporter gene expression is regulated by the endogenous *Pbsdha* gene promoter (Fig. 2A). It is reported that the first 60 amino acids of *P. falciparum* Fp (PfFp) contain a functional mitochondrial targeting signal (*21*) and the corresponding amino acid sequence of PbFp shows 75% identity to that of PfFp (*11*), suggesting the same function in the corresponding region of PbFp. To investigate the cellular localization and developmental expression of AGFP during the parasite life cycle, the first 60 amino acids of PbFp was fused to AGFP (Pbsdha::AGFP). The WT parasites were transfected with the *Pbsdha::AGFP* plasmid and the correct integration event in Pbsdha::AGFP parasite clone was confirmed by Southern blot (Fig. 2B). For the analysis of cellular localization of AGFP, the Pbsdha::AGFP parasites were stained with MitoTracker Orange to label the mitochondrion. As shown in Fig. 2C, AGFP signals colocalized with MitoTracker Orange signals, indicating that the N-terminal sequence of PbFp possesses a functional mitochondrial targeting signal. Next, we investigated the reporter gene expression at each developmental stage of parasites in red blood cell. AGFP signal was detected in trophozoite and schizont (Fig. 2D) but not in the ring form stage (data not shown). To investigate the AGFP expression in the parasites at mosquito stages, Pbsdha::AGFP parasites were fed to mosquitoes. As shown in Fig. 2E, the signal was detected in *in vitro*-cultured ookinetes, and oocysts and sporozoites in mosquitoes. These results indicate that *Pbsdha* was expressed in both blood stages and mosquito stages.

Disruption of the Pbsdha gene

Then, to study the *P. berghei* complex II functions, we generated Pbsdha(-) parasites by replacing the *Pbsdha* gene with *TgDHFR* (Fig. 3A). Two independent clones (KO-a and KO-b) were established by independent transfection experiments. The correct targeting event in each clone was confirmed by Southern blot analysis (Fig. 3B) and diagnostic PCR (Fig. 3C). Following the confirmation of *Pbsdha* gene disruption, we further checked the deletion of the PbFp protein and SQR enzyme activity in Pbsdha(-) parasites by Western blot and enzyme activity assay, respectively. For these experiments, we prepared the crude mitochondrial samples from WT, Pbsdha(-) parasites, *in vitro* cultured *P. falciparum*, and naïve mouse liver. To detect the Fp peptide by Western blot analysis, we used the anti-PfFp antiserum (*20*) because the amino acid sequence of PfFp shows high identity to those of PbFp (90.5 %) and mice Fp (63.3 %). It is thus anticipated that the antiserum may cross-react to both PbFp and mice Fp proteins. As shown in Fig. 3D, the antiserum reacted to the peptides with expected size of

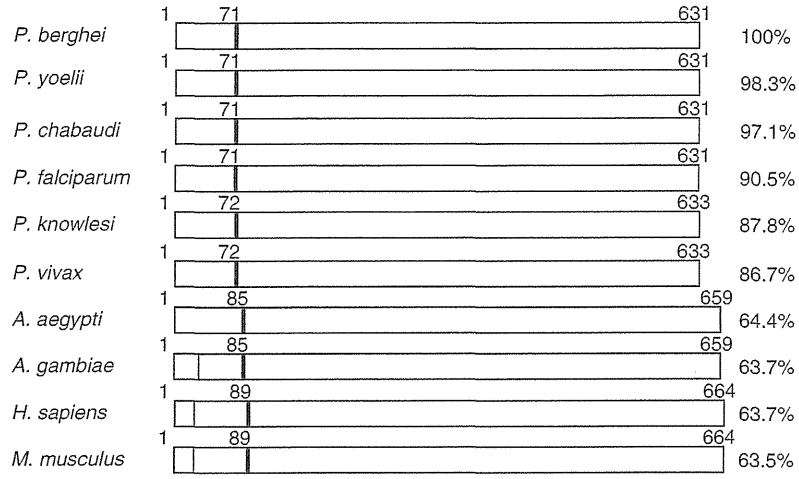

Fig. 1 Primary structure of Fp proteins from 10 species. The box indicates the full-length Fp protein. The mitochondrial sorting signal is colored in grey. The black line with number indicates the conserved His for FAD binding site. The total number of amino acid residues and the amino acid identity to PbFp are indicated on the right (%).

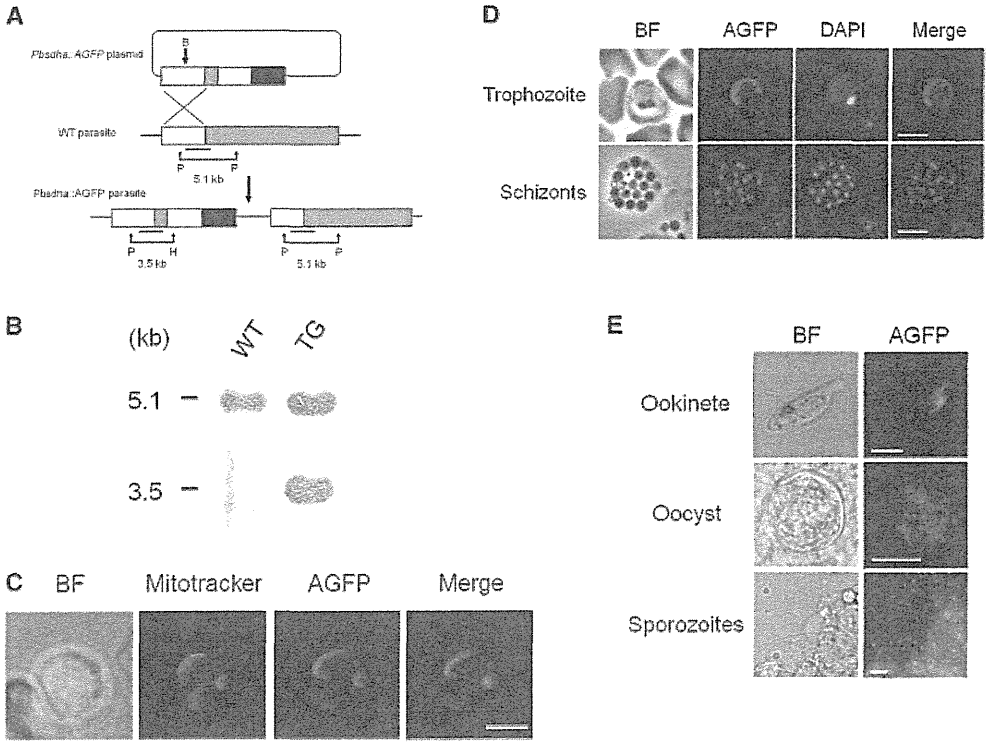

Fig. 2 Generation of the transgenic parasite line Pbsdha::AGFP. (A)Schematic representation of *AGFP* tagging of the *Pbsdha* locus using a plasmid that integrated through single crossover homologous recombination. In the *Pbsdha::AGFP* plasmid, the boxes indicate *Pbsdha* gene promoter (white), the first 60 amino acids of Pbsdha (dark gray), AGFP (light gray), 3'UTR of *Pbsdha* gene and *TgDHFR/ts* selectable marker cassette (black). In the *Pbsdha* gene locus (middle), the box with dark gray indicates full open reading frame of *Pbsdha*. B, H and P indicate *BstXI*, *HpaI* and *PacI* digestion sites, respectively. Bars represent the position of the probe used in Southern blot analysis. (B) Southern blot analysis of WT and Pbsdha::AGFP parasites. Hybridization of the probe with *PacI*- and *HpaI*-digested genomic DNA yielded a 5.1 kb for WT, and 3.5 kb and 5.1 kb for Pbsdha::AGFP parasites (TG). (C) Cellular localization of AGFP in Pbsdha::AGFP parasites. The mouse erythrocyte infected with Pbsdha::AGFP parasites was observed under bright field (BF). The signals of MitoTracker and AGFP in the same cell were detected through red (MitoTracker) and green filter (AGFP), respectively. Bar represents 5 μm. (D) Expression of *AGFP* gene in Pbsdha::AGFP parasites at blood stages. The AGFP signal was detected in the parasites synchronized at trophozoite (upper) and schizont stages (lower). Nuclei were stained with DAPI. Bars represent 5 μm. (E) Expression of the *AGFP* gene in Pbsdha::AGFP parasites at mosquito stages. The AGFP signal was detected in *in vitro* cultured-ookinetes, oocysts in the midguts and sporozoites in the salivary gland of mosquitoes. Bar represents 20 μm.

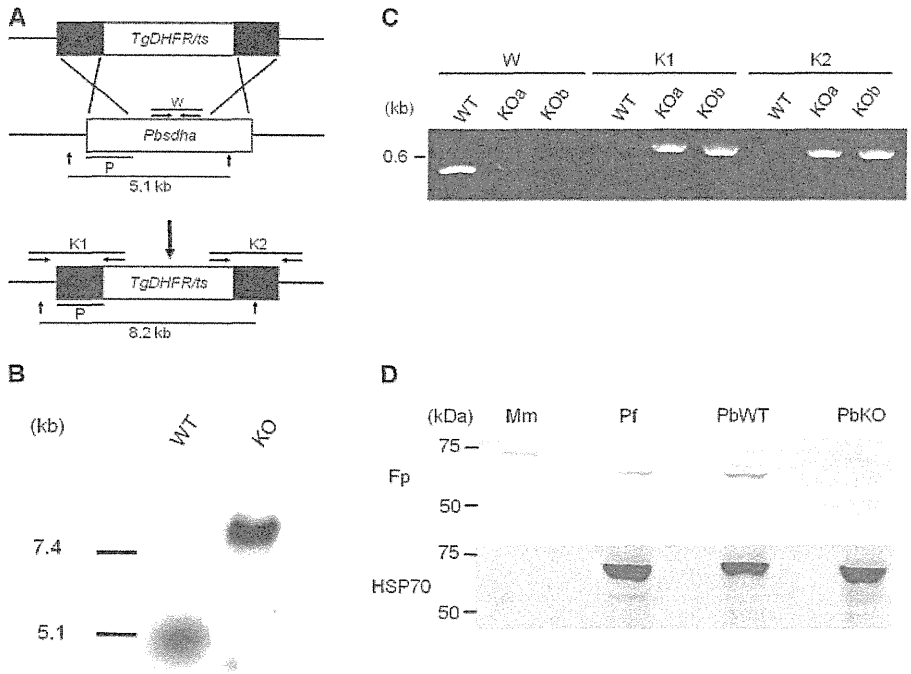

Fig. 3 Targeted disruption of the *Pbsdha* gene. (A) Schematic representation of the replacement strategy to generate Pbsdha(-) parasites. The WT *Pbsdha* gene locus is replaced with 5′ and 3′ UTRs of the *Pbsdha* gene and *TgDHFR*, a selectable marker. Vertical arrows indicate *PacI* site. P with bar indicates the probe position for Southern blot analysis. Arrows marked with W (WT specific) or K1/K2 (knockout specific) indicate the primer positions used in diagnostic PCR. (B) Southern blot genotyping confirmed integration. Hybridization of the probe with *PacI*-digested genomic DNA of WT and Pbsdha(-) parasites yielded a 5.1 kb and 8.2 kb band, respectively. (C) Confirmation of *Pbsdha* gene disruption by diagnostic PCR. Genomic DNA from WT, Pbsdha(-) clone A (KOa) and clone B (KOb) were used as templates. The positions of the PCR products in W and K1/K2 are depicted in Fig. 2A. (D) Detection of Fp peptides by Western blot analysis. The Fp peptides in mitochondrial fractions of *Mus musculus* (Mm), *P. falciparum*(Pf), *P. berghei* wild-type (PbWT) and Pbsdha(-) (PbKO) parasites were detected by anti-PfFp antiserum (upper panel). The anti-PbHSP70 antiserum was used to confirm equal loading of the protein samples in each lane (lower panel).

70.5 kDa (WT *P. berghei*) and 73.0 kDa (mice), as well as 70.7 kDa (*P. falciparum*). In contrast, no band was detected in Pbsdha(-) (PbKO) except for the high molecular weight band, which is speculated as contaminated mice Fp because the molecular weight of this faint band is similar to that of the band on Mm lane (Fig. 3D). The equal loading of each sample on the gel was confirmed by anti-PbHSP70 antiserum (lower panel in Fig. 3D). These results demonstrated that the PbFp protein was surely deleted from Pbsdha(-) parasites. Next, we investigated the SQR activity in Pbsdha(-) parasites by using the same samples used for Western blot analysis. While WT parasites showed an SQR activity of 4.38 ± 0.96 nmol/min/mg ($N=3$), Pbsdha(-) did not show any detectable SQR activity (Table I). These results demonstrated that the PbFp protein and the SQR activity were completely eliminated from the Pbsdha(-) parasites.

Phenotypic analysis of Pbsdha(-) parasites

As the disruption of the *Pbsdha* gene was confirmed, phenotypic effect of the gene disruption on the parasite was analyzed. In erythrocytic stages, Pbsdha(-) parasites underwent normal development and differentiation into gametocytes, which were not significantly different from those of WT parasites ($P>0.1$, Fig. 4 and Table II). Successful *Pbsdha* gene deletion indicates that the SQR enzyme is not essential for the survival of the parasite at asexual stages and sexual differentiation. The mitochondria of Pbsdha(-) parasites were stained with Mitotracker, indicating that disruption of *Pbsdha* did not affect the mitochondrial membrane potential (Fig. 5).

Next, we investigated the parasite development at mosquito stages. In *P. berghei*, an *in vitro* assay has been established that mimics the gametogenesis and fertilization taking place in the mosquito body (*22*). Using this system, we confirmed that the efficiency of male gametogenesis in Pbsdha(-) parasites was comparable with that of WT parasites (data not shown). However, Pbsdha(-) parasites showed severe defects in ookinete formation, the stage next to fertilization. The conversion rate of female gametes to ookinetes in Pbsdha(-) was significantly reduced to 17% of WT parasite ($P<0.05$ ($N=3$), Fig. 6A). We further investigated the infectivity of Pbsdha(-) parasites to mosquitoes and the subsequent transmission to mice. The mosquitoes were fed on mice carrying either Pbsdha(-) or WT parasites, and then these mosquitoes were dissected for the evaluation of parasite development at day 16 post-feeding. Interestingly, several independent experiments using two clones showed that no oocysts were detected in the midguts of mosquitoes fed on mice carrying Pbsdha(-) parasites, while oocysts

Table I. SQR activity of the mitochondrial fraction in WT and Pbsdha(-) parasites.

	Exp 1	Exp 2	Exp 3
WT	5.31	4.44	3.40
KO	0.00	0.00	0.00

The value represents SQR activity in each independent assay (nmol/min/mg protein)

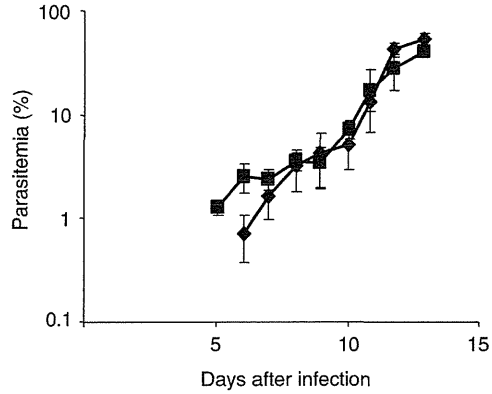

Fig. 4 The growth rate of intraerythrocytic stages of WT and Pbsdha(-) parasites. The parasitemia of WT and Pbsdha(-) parasites are indicated by closed square and diamond, respectively. Bar represents SD (N = 4).

Table II. The gametocytemia of WT and Pbsdha(-) parasites.

Parasites	Macrogametocytemia/ parasitemia	Microgametocytemia/ parasitemia
WT	6.5 ± 2.72	1.7 ± 0.45
KO	5.0 ± 1.11	1.5 ± 0.64

were detected in the mosquitoes fed on mice carrying WT parasites (Fig. 6B). Moreover, no transmission was observed in the mice challenged by the mosquitoes carrying Pbsdha(-) parasites, while WT parasites were transmitted to mice (Table III). Taken together, these results indicated that the development of Pbsdha(-) parasites was completely halted at the stage of oocyst formation.

Discussion

It is known that asexual stages parasites possess a single acristate mitochondria, while gametocytes, mosquito stages and preerythrocytic stage parasites possess five to six cristate mitochondria (*9*, *23*). This morphological maturation of mitochondria in the sexual stage parasites may correlate with the increased need of mitochondrial metabolism in the insect stage parasite development. Once malaria parasites are introduced to mosquitoes, they encounter to drastic environmental changes where the main sugar source is changed from glucose to torehalose, and they need to adapt to this (*24*). Our present work clearly shows that complex II has a critical role in parasite adaptation to the insect body. Namely, the parasite lacking complex II activity failed to form oocysts in mosquitoes, while the development of blood stage parasites in mice was not affected by *Pbsdha* gene disruption at all.

Developmental expression and targeting disruption of Pbsdha gene

By using Pbsdha::AGFP parasites as a reporter, we followed the AGFP expression during the whole parasite life cycle except for liver stage. Except for the ring stage, AGFP signals were detected in all developmental stages. It was reported that the size and morphology of mitochondria spectacularly changes during the life cycle and that the mitochondrial size is much smaller in the ring stage than in any other stage (*25*). Thus, the failure of signal detection in ring stage could be attributed to lower signal strength than the detection limit. According to gene expression data in PlasmoDB, the *P. falciparum* orthologous gene of *Pbsdha*, PF10_0334 is substantially expressed in all developmental stages including the ring form. Taken together, it can therefore be speculated that the *Pbsdha* gene is also expressed in all developmental stages.

In a global gene expression analysis, it was reported that several lines of *in vitro*-cultured *P. falciparum* showed very similar pattern in gene expression. In contrast, it was recently demonstrated that parasites derived directly from infected patients showed three distinct gene expression states (*26*). One of these states showed that the expression levels of *sdha* and other TCA cycle- or ETC-related genes are increased. Because such expression state has never been detected in *in vitro* studies and parasitic mitochondria are immature acristates, it had been considered that the blood-stage parasites mainly use cytosolic glycolysis and mitochondrial oxidative phosphorylation only marginally (Fig. 7). The discrepancy between the *in vivo* and *in vitro* studies above suggests that the parasites may use oxidative phosphorylation in *in vivo* in case that the patient would be hypoglycemic, which is reflected in the upregulation of the genes involved in oxidative phosphorylation. In the *in vitro* system, on the other hand, glucose is continuously supplied in the medium and the environmental condition is artificially controlled, therefore the parasites may exclusively undergo glycolysis and the enzymes of oxidative phosphorylation may be marginally expressed. Thus, it is important to undertake experiments using both *in vitro* and *in vivo* systems in order to understand how parasites respond to various environmental stimuli. In this sense, the rodent malaria model could be an ideal tool to investigate the changes in parasite metabolism *in vivo*.

Complex II is essential for the parasite survival at mosquito stages

We successfully generated Pbsdha(-) parasites, confirmed by Southern blot, diagnostic PCR and SQR activity assay. It is anticipated that the mitochondrial membrane potential was decreased in Pbsdha(-) parasites as a result of the knockout. Unexpectedly, the

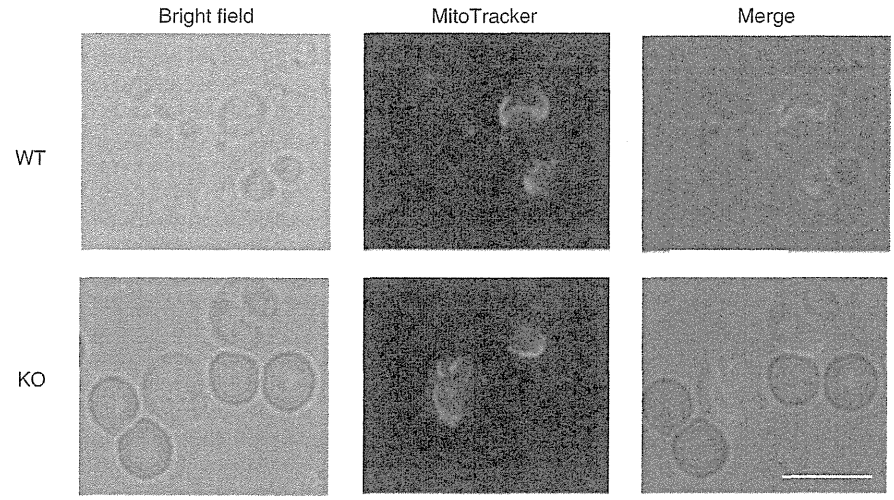

Fig. 5 MitoTracker staining of WT and Pbsdha(-) parasites. The erythrocytes infected with WT or Pbsdha(-) (KO) parasites was stained with MitoTracker to assess the integrity of the mitochondrial membrane potential. Bar represents 5 μm.

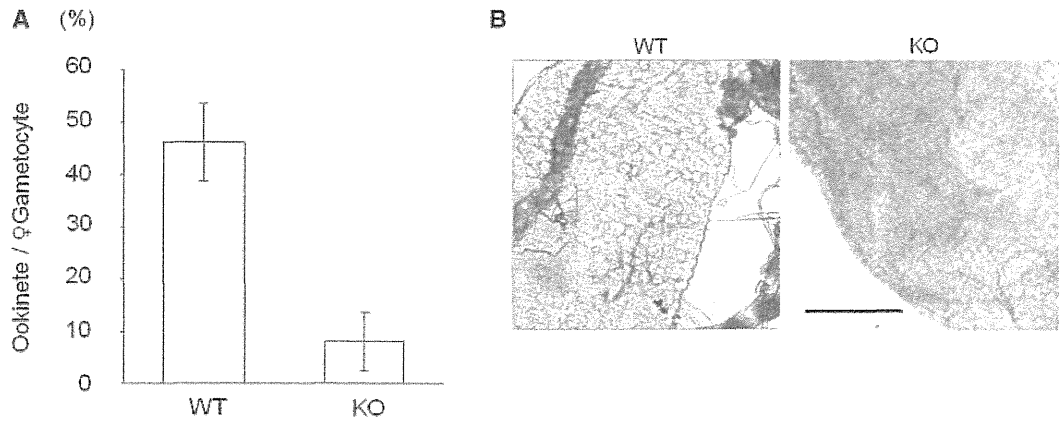

Fig. 6 Phenotypic analysis of Pbsdha(-) parasites. (A) Ookinete formation rate of WT and Pbsdha(-) (KO) parasites. The mouse blood infected with either WT or Pbsdha(-) parasites was incubated in fertilization medium to induce fertilization and differentiation into ookinetes. The ookinete formation rate was calculated by the percentage of female gametocytes, which converted into ookinetes. Error bars represents mean ± SD (n = 3). (B) Mosquito midguts infected with WT and Pbsdha(-) (KO) parasites. The latter carries no oocyst. Bars represent 200 μm.

Table III. Infectivity of WT and Pbsdha(-) parasites.

Parasite		Oocyst-positive mosquitoes	Mean oocysts/ midgut ± SD	Mouse infection
WT	Exp1	7/21	5.4 ± 11.3	+
	2	6/20	7.3 ± 6.4	+
	3	5/20	18.0 ± 30.3	+
	4	13/20	25.1 ± 30.5	+
	5	15/32	51.8 ± 63.4	+
Koa	Exp1	0/20	0	−
	2	0/20	0	−
	3	0/20	0	−
	4	0/20	0	−
	5	0/20	0	−
	6	0/20	0	−
Kob	Exp1	0/26	0	−

mitochondrial membrane potential seemed to be maintained in blood-stage parasites in the absence of complex II, which was demonstrated by the positive signal in MitoTracker staining. In addition to complex II, there are three other enzymes involved in electron flux that contribute to mitochondrial membrane potential; MQO (malate–quinone oxidoreductase), DHOD (dihydroorotate dehydrogenase) and NDH2 (type2 NADH–ubiquinone oxidoreductase), which is a single peptide dehydrogenase different from multi-subunit complex I (Fig. 7). It is therefore conceivable that any of these three enzymes may be a functional complement for the absence of complex II. Recently, it was reported that *P. berghei* lacking NDH2 (NDH2(-)) did keep mitochondrial membrane potential (*27*), supporting the hypothesis of mutual complementation among ETC enzymes.

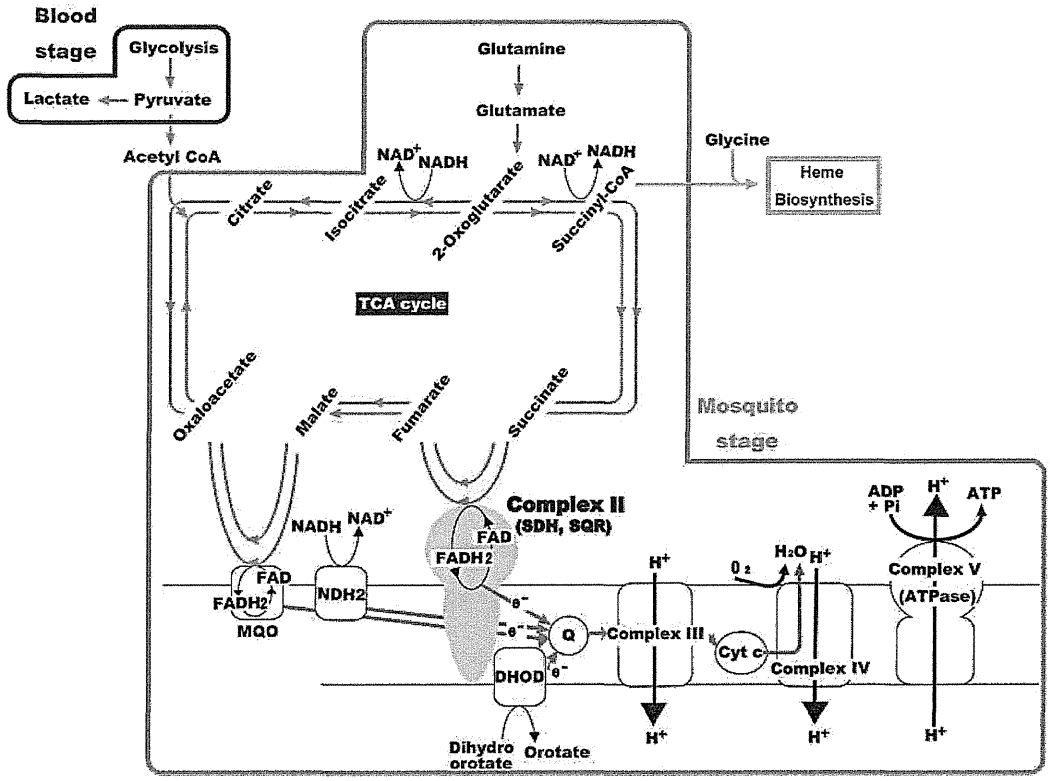

Fig. 7 Hypothetical Model of Plasmodial energy metabolism. Blue arrows represent canonical flow of glycolysis and TCA cycle. Green arrows represent *Plasmodium* TCA metabolism pathway. Unlike other eukaryotes, glycolysis (enclosed by red) does not link to TCA cycle. *Plasmodim* TCA cycle is initiated by uptaking of glutamine into mitochondria. Mitochondrial oxidative phosphorylation (enclosed by green) is essential for the parasite survival at mosquito stage because the Pbsdha(-) parasite is lethal at this stage.

Our phenotypic study revealed that Pbsdha(-) parasites proliferated and produced gametocytes with a similar rate to WT parasites in mice. Recently, we observed similar results in the blood-stage *P. falciparum*, of which Fp subunit was disrupted (Tanaka *et al.*, submitted for publication). *In vitro*, Pbsdha(-) male gametocytes differentiated to gametes (exflagellated) as WT ones, suggesting that complex II is not required for those developmental stages. It is known that mammalian sperm requires ATP for flagellum movement, which is supplied mainly from mitochondrial oxidative phosphorylation (*28*). While male gametes of malaria parasites show similar motility to that of mammalian sperm, it is obvious that parasite male gametes do not rely on oxidative phosphorylation because the male gametes do not possess mitochondria (*24*). This indicates that the driving force for male motility is exclusively supplied from glycolysis. The *in vitro* fertilization assay showed that Pbsdha(-) parasites were defect in ookinete formation. At this moment, it is not clear whether complex II is critical at female gametogenesis, fertilization or ookinete formation itself. Nevertheless, we speculate that the impact of *Pbsdha* gene disruption gave adverse influence on female, probably the stages after gametocytogenesis.

The most drastic phenotypic change in Pbsdha(-) parasites was the complete failure of oocyst formation. In malaria parasites, the ookinetes traverse midgut cell and arrive to the basal lamina where they transform into oocysts. In a single oocyst, mitosis occurs and several hundreds of sporozoites are generated inside. To accomplish such task, the parasites may need more ATP, which could be generated by oxidative phosphorylation. The complex II activity deletion may therefore adversely affect the oocyst formation. Recently, it was reported that NDH2(-) parasites developed normally in asexual stages but transformed into aberrant immature oocysts (*27*). Our present study together with this finding suggests that the ETC enzymes are essential in insect stages. However, there are several phenotypic differences between Pbsdha(-) and NDH2(-) parasites; 1) Pbsdha(-) parasites differentiated into ookinetes with low efficiency, while NDH2(-) ookinete formation is similar to WT parasites. This indicates that the Pbsdha deletion affects an earlier parasite stage compared with that of NDH2 deletion; 2) Pbsdha(-) parasites failed completely in oocyst formation, while NDH2(-) parasites formed immature oocysts with smaller size, demonstrating that the absence of complex II gives more severe defects in parasite development than NDH2 does. In other eukaryotes, it is known that mitochondrial complex II converts succinate to fumarate and reducing equivalents are transferred to quinone. In addition, complex II is one of the TCA cycle members

generating NADH, which is a substrate of NDH2. Thus, the deletion of complex II activity may render NDH2 unable to function in ETC. Severe phenotypic changes in Pbsdha(-) parasites could be therefore attributed to the aberration of NDH2 as well as complex II itself.

Conclusion

In the present work, we show that complex II has a critical role in insect-stage parasites. ETC is not only involved in ATP metabolism, but as well in heme biosynthesis (Fig. 7), which is also crucial for parasite survival (*29*). In addition to the ETC, complex II functions as the TCA cycle enzyme. Further studies are required to determine whether lack of any of these functions are the cause for the developmental arrest in Pbsdha(-) parasites. In any case, our study demonstrates that malaria parasite drastically switches energy metabolism when the parasites initiate sexual maturation and is subsequently introduced into the mosquito (Fig. 7).

The importance of complex II in insect-stage parasites suggests the possibility that complex II could be a novel target for transmission blocking (*30*). Previously, we reported that the amino acid sequences of the membrane anchor subunits CybL and CybS of *Plasmodium* complex II show exceptionally low homology to that of any other organism including human (*12*). In addition, our previous work revealed that atopenin A5 is a potent inhibitor against mammalian complex II with IC_{50} values of three-order of magnitudes lower than that of *Plasmodium* complex II (*13*). This indicates that 3D structure of ubiquinone-binding site in the parasitic complex II is quite distinct from those of mammalian complex II. Therefore, it is conceivable that the development of a parasitic complex II-specific inhibitor would be feasible by structure-based drug design targeting to the mosquito-stages parasite. Currently, further ATP metabolic gene knockout experiment using mouse malaria models are now in progress to draw general view of parasite energy metabolism in response to various environmental stimuli that may have been overlooked in *in vitro* culture systems as pointed out by Daily (*31*).

Acknowledgements

We thank Dr. Terenius for his comments on our manuscript.

Funding

Grants-in-aid for Creative Scientific Research (18GS0314 to KKand YW) and for Scientific Research (C) (21590467 to YY and 20590426 to MH) from the Japanese Society for the Promotion of Science, Targeted Proteins Research Program (to KK) and a Grant-in-aid for Scientific Research on Priority Areas (18073004 to KK and 210220044 to MH) and Grant-in-Aid for Scientific Research on Innovative Areas (22112519 to MH) from the Japanese Ministry of Education, Science, Culture, Sports and Technology, and a grant for research to promote the development of anti-AIDS pharmaceuticals from the Japan Health Sciences Foundation (to KK). This work was also partially suppored by Support Program for Scientific Research Platform in Private Universities (to HM) and SUMITOMO foundation (to MH).

Conflict of interest

None declared.

References

1. Snow, R.W., Guerra, C.A., Noor, A.M., Myint, H.Y., and Hay, S.I. (2005) The global distribution of clinical episodes of *Plasmodium falciparum* malaria. *Nature* **434**, 214–217
2. Petersen, I., Eastman, R., and Lanzer, M. (2011) Drug-resistant malaria: molecular mechanisms and implications for public health. *FEBS Lett.* **585**, 1551–1562
3. Foth, B.J., Stimmler, L.M., Handman, E., Crabb, B.S., Hodder, A.N., and McFadden, G.I. (2005) The malaria parasite *Plasmodium falciparum* has only one pyruvate dehydrogenase complex, which is located in the apicoplast. *Mol. Microbiol.* **55**, 39–53
4. Aikawa, M. (1966) The fine structure of the erythrocytic stages of three avian malarial parasites. *Plasmodium fallax, P. lophurae, and P. cathemerium. Am. J. Trop. Med. Hyg* **15**, 449–471
5. Bryant, C., Voller, A., and Smith, M.J. (1964) The incorporation of radioactivity from (14C)glucose into the soluble metabolic intermediates of malaria parasites. *Am. J. Trop. Med. Hyg* **13**, 515–519
6. Scheibel, L.W. and Pflaum, W.K. (1970) Cytochrome oxidase activity in platelet-free preparations of *Plasmodium falciparum. J. Parasitol.* **56**, 1054
7. Olszewski, K.L., Mather, M.W., Morrisey, J.M., Garcia, B.A., Vaidya, A.B., Rabinowitz, J.D., and Llinas, M. (2010) Branched tricarboxylic acid metabolism in *Plasmodium falciparum. Nature* **466**, 774–778
8. Hall, N., Karras, M., Raine, J.D., Carlton, J.M., Kooij, T.W., Berriman, M., Florens, L., Janssen, C.S., Pain, A., Christophides, G.K., James, K., Rutherford, K., Harris, B., Harris, D., Churcher, C., Quail, M.A., Ormond, D., Doggett, J., Trueman, H.E., Mendoza, J., Bidwell, S.L., Rajandream, M.A., Carucci, D.J., Yates, J.R. 3rd, Kafatos, F.C., Janse, C.J., Barrell, B., Turner, C.M., Waters, A.P., and Sinden, R.E. (2005) A comprehensive survey of the *Plasmodium* life cycle by genomic, transcriptomic, and proteomic analyses. *Science* **307**, 82–86
9. Krungkrai, J., Prapunwattana, P., and Krungkrai, S.R. (2000) Ultrastructure and function of mitochondria in gametocytic stage of *Plasmodium falciparum. Parasite* **7**, 19–26
10. Maklashina, E. and Cecchini, G. (2010) The quinone-binding and catalytic site of complex II. *Biochim. Biophys. Acta.* **1797**, 1877–1882
11. Takeo, S., Kokaze, A., Ng, C.S., Mizuchi, D., Watanabe, J.I., Tanabe, K., Kojima, S., and Kita, K. (2000) Succinate dehydrogenase in *Plasmodium falciparum* mitochondria: molecular characterization of the SDHA and SDHB genes for the catalytic subunits, the flavoprotein (Fp) and iron-sulfur (Ip) subunits. *Mol. Biochem. Parasitol.* **107**, 191–205
12. Mogi, T. and Kita, K. (2009) Identification of mitochondrial Complex II subunits SDH3 and SDH4 and ATP synthase subunits a and b in Plasmodium spp. *Mitochondrion* **9**, 443–453
13. Kawahara, K., Mogi, T., Tanaka, T.Q., Hata, M., Miyoshi, H., and Kita, K. (2009) Mitochondrial dehydrogenases in the aerobic respiratory chain of the rodent malaria parasite *Plasmodium yoelii yoelii. J. Biochem.* **145**, 229–237
14. Takashima, E., Takamiya, S., Takeo, S., Mi-ichi, F., Amino, H., and Kita, K. (2001) Isolation of